water

MDPI

Article

Assessing the Effects of Opencast Coal Mining on the Quality of Surface Water: A Case Study in the Leeuwfonteinspruit, a Tributary of the Olifants River

Clement Moswine Mogofe [1,*], Gladys Belle [2] and Paul Oberholster [2]

[1] Centre for Environmental Management, Faculty of Natural and Agricultural Sciences, University of the Free State, Bloemfontein 9300, South Africa
[2] Centre for Mineral Biogeochemistry, Faculty of Natural and Agricultural Sciences, University of the Free State, Bloemfontein 9300, South Africa; belle.gn@ufs.ac.za (G.B.); oberholsterpj@ufs.ac.za (P.O.)
* Correspondence: 2021679903@ufs4life.ac.za; Tel.: +076-642-1531

Abstract

Assessing the effects of opencast coal mining on surface water is often complex, requiring integrated approaches that combine guideline-based assessments, water quality indices (WQIs), hydrochemical tools, and statistical analyses. This study evaluated multi-year water quality data (2018–2023) from five sites along the Leeuwfonteinspruit, a tributary of the Olifants River Catchment in the Mpumalanga Province, South Africa. Water quality parameters were assessed against the South African Water Quality Guidelines (SAWQGs) for domestic, agricultural, and aquatic ecosystem uses. The results indicate frequent exceedances of SAWQGs for key parameters such as sulfate (SO_4), electrical conductivity (EC), total dissolved solids (TDS), magnesium (Mg), calcium (Ca), iron (Fe), aluminum (Al), and manganese (Mn), particularly at the downstream site. Weighted Arithmetic Water Quality Index (WA-WQI) and Canadian Council of Ministers of the Environment Water Quality Index (CCME-WQI) classified water quality from good at some upstream sites to consistently poor or marginal water quality at downstream sites. Irrigation assessments based on sodium adsorption ratio (SAR), sodium percentage (Na%), and the United States Salinity Laboratory (USSL) diagram indicated that surface water posed a low sodicity risk across the catchment, with salinity identified as the primary constraint to irrigation suitability. Hydrogeochemical evaluation using Gibbs diagrams suggested that the upstream water chemistry is dominated by natural rock–water interactions and dilution processes, while midstream to downstream sites increasingly exhibit characteristics consistent with evaporation–crystallization and anthropogenic influences. Principal Component Analysis (PCA) and correlation analysis further suggested that water quality patterns are largely associated with salinity and mineralization that may be influenced by mining activities, with secondary contributions from agricultural inputs. Overall, the findings suggest that opencast coal mining is an important contributor to surface water quality deterioration in the Leeuwfonteinspruit, although other catchment activities and natural geochemical processes may also contribute. These findings highlight the need for strengthened monitoring, proactive mine water management, and effective regulatory enforcement.

Keywords: opencast coal mining; surface water pollution; Olifants river; water quality index; multivariate statistical analysis; sodium adsorption ratio; sodium percentage; Sequential Mann–Kendall; Gibbs diagram

Check for updates

Academic Editor: Christos S. Akratos

Received: 11 May 2026
Revised: 6 July 2026
Accepted: 23 July 2026
Published: 1 September 2026

Copyright: © 2026 by the authors. Licensee MDPI, Basel, Switzerland. This article is an open access article distributed under the terms and conditions of the Creative Commons Attribution (CC BY) license.

1. Introduction

Despite significant advancements in renewable energy sources such as wind, photovoltaic, hydropower, and natural gas, coal continues to dominate the global power production sector, driving infrastructural development and economic growth worldwide [1–3]. However, coal mining and processing have significantly impacted the environment by destroying habitats [4], polluting water resources [5,6], and causing soil erosion [7]. These activities have also adversely impacted human health through the release of harmful pollutants, such as coal dust and toxic chemicals, which can lead to respiratory problems and other serious illnesses [8]. Furthermore, the burning of coal for energy has resulted in the release of greenhouse gases that contribute to climate change [9–11].

Extensive research has examined the impacts of coal mining on water resources globally, including studies in India [7], the United States [3], China [12], Nigeria [13], and Australia [14]. Reported impacts of coal mining on water resources include the destruction of aquifers, formation of acid mine drainage, and contamination of both groundwater and surface water systems [10,15–17]. However, most studies have focused on large rivers, reservoirs, and regional catchments, while comparatively little attention has been given to smaller tributaries that receive direct inputs from mining activities. Small tributaries are particularly vulnerable to contamination because of their limited dilution capacity, rapid hydrological response, and proximity to pollution sources. Consequently, they often represent the first receptors of mining-derived contaminants and serve as important pathways for the downstream transport of pollutants. Since water has no substitute, understanding and protecting these vulnerable systems is essential for sustainable water resource management [18].

South Africa continues to rely significantly on coal for its economic development and energy security [19,20]. The Mpumalanga Province, which hosts 80% of the country's coal mines, is the epicenter of coal supply in South Africa [21]. The Highveld and Witbank coalfields in Mpumalanga, located within the Olifants River Catchment, constitute the largest region of active coal mining operations in the country, significantly contributing to the river's designation as one of the most polluted in southern Africa [22]. The Catchment, covering approximately 85,000 km^2, spans segments in both Mozambique and South Africa [23], is of strategic importance because it supports domestic, agricultural, industrial and ecological water demands. The deterioration of water quality and availability due to irresponsible mining practices further exacerbates South Africa's water scarcity challenges and poses a growing concern to water security [21].

Among the various mining methods, opencast coal mining is widely utilized in South Africa due to its cost efficiency and high recovery rates [24,25]. However, this mining method poses significant threats to already stressed water resources [26]. The primary sources of surface water pollution in opencast coal mining include dewatering of mine-affected water, wastewater from dust suppression systems, seepage during excavations, and leachate runoff from waste dumps, processing plants, and product stockpiles [17]. Additional contamination arises from acid mine drainage generated by exposed sulfide minerals, sediment-laden runoff from disturbed land, explosives residues from blasting, and accidental spills of fuels and chemicals [27].

The assessment of physicochemical parameters in mining areas provides insights into contamination sources and potential environmental impacts [18,28,29]. Due to the complexity of parameters involved in surface water quality assessment, various statistical analyses and hydrochemical tools have been developed to interpret water quality data. Hydrochemical tools, such as SAR, Na%, WQIs, and Gibbs diagrams, are commonly used to evaluate water quality, identify potential pollution risks, determine irrigation suitability, and understand dominant hydrochemical processes [28,30–32]. Similarly, multivariate

statistical analysis, such as cluster analysis, PCA, factor analysis, correlation analysis, and Sequential Mann–Kendall (SMK) analysis, are frequently used to categorize contamination sources, detect spatial and temporal trends, and explore relationships between key water quality parameters [33–37].

Despite well-documented impacts of coal mining on the Olifants River [22,38–41], there is a notable lack of studies investigating how opencast coal mining activities affect smaller tributaries, such as Leeuwfonteinspruit, that directly feed into the Olifants River and affect the health of downstream water users. These tributaries play a critical role in the overall health of the catchment, acting as conduits that transport pollutants from mining sites to larger water bodies. Their degradation can further lead to long-term ecological consequences, affecting biodiversity, human livelihoods, and water security. Furthermore, few studies have comprehensively evaluated the spatial and temporal variability of water quality, irrigation suitability, and long-term trends in these mining-impacted tributaries using an integrated approach. This leaves a crucial gap in our understanding of localized pollution sources and limits the development of effective management and mitigation strategies aimed at protecting downstream water users and aquatic ecosystems.

To address these knowledge gaps, the present study examined the Leeuwfonteinspruit, a tributary of the Olifants River, to evaluate the effects of opencast coal mining activities on surface water quality. By analyzing temporal and spatial variations in key water quality parameters and identifying potential sources of contamination, the research provided a scientific basis for understanding how mining activities affect downstream water users and ecosystem integrity. The objectives of the study were to (1) determine the current water quality status of the stream, (2) analyze spatial and temporal trends across the monitoring sites, (3) investigate the potential sources and pathways of contamination, (4) assess the suitability of the water for downstream users, and (5) develop management and mitigation strategies to protect downstream water users.

2. Materials and Methods

2.1. Study Area

The study area is located within the Mpumalanga Province of South Africa, approximately 23 km west of Hendrina and 40 km south of Middelburg. It falls within the upper Olifants River Catchment, specifically within quaternary catchment B11B, which includes the Leeuwfonteinspruit. This catchment falls within the larger Limpopo River Basin, an international drainage system shared by South Africa, Zimbabwe, Botswana, and Mozambique [23].

The upper section of the Olifants River flows into the Witbank Dam, which subsequently drains into the Doornpoort Dam. The water from the Witbank Dam is utilized for both industrial and domestic purposes. In addition, the dam serves as key recreational site, supporting activities such as birdwatching, fishing, camping, sailing, boating and other leisure activities along its banks.

The Leeuwfonteinspruit catchment area is characterized by primarily grassland natural vegetation, alongside widespread irrigated and dry-land agricultural activities. Livestock farming in various forms is also prevalent. The area is dotted with several small towns and smaller urban settlements, predominantly serving as satellite communities for the nearby coal mines and power stations dispersed throughout the region. Figure 1 indicates the study area in relation to the quaternary catchments, surrounding towns and major tributaries of the Olifants River.

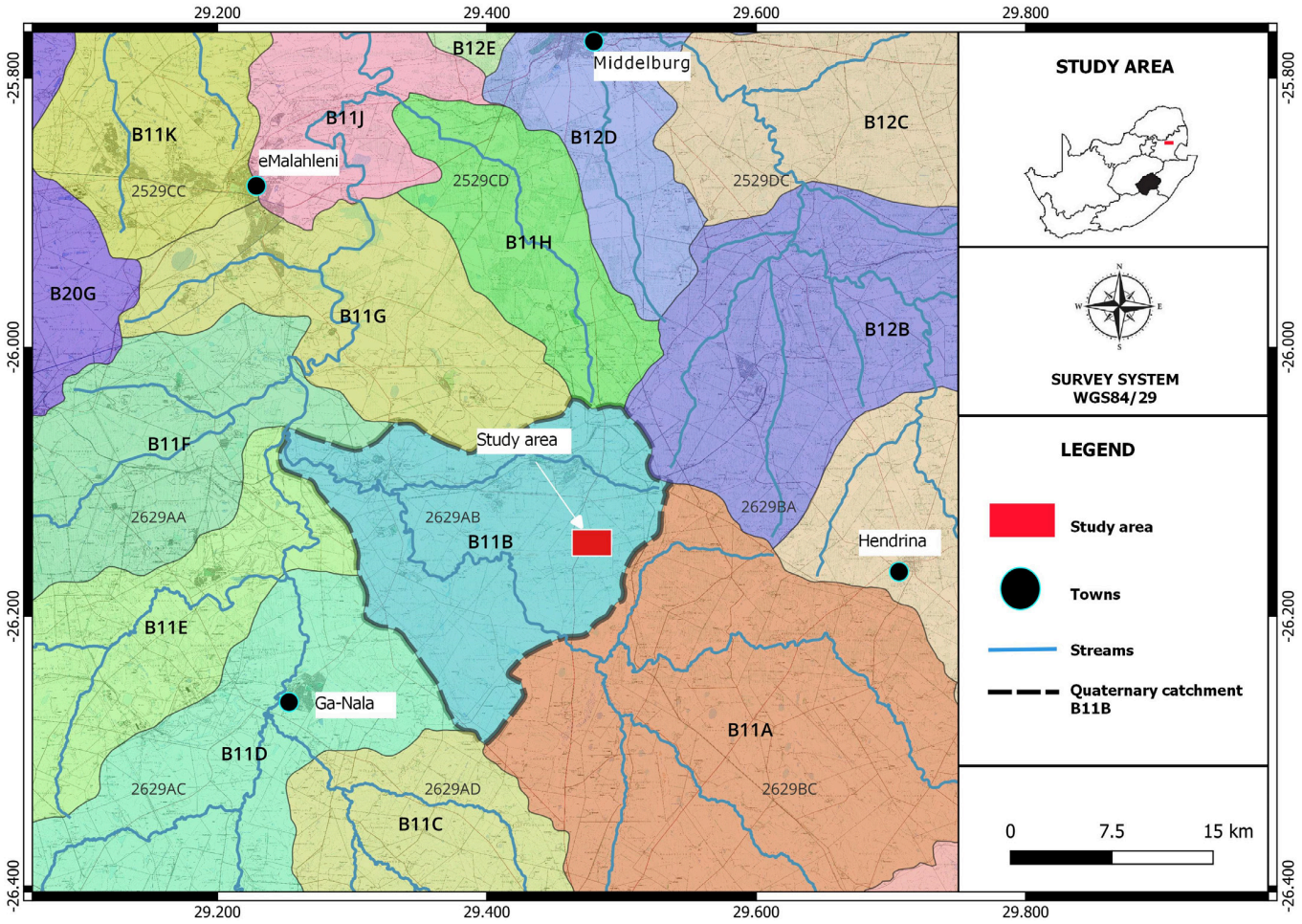


Figure 1. Map of the study area showing the quaternary catchments and surrounding towns.

The study area is characterized by extensive opencast coal mining activities, where groundwater is continuously pumped from the pits to pollution control dams to maintain dry working conditions. This dewatering process lowers groundwater levels within the mined strata, alters natural groundwater flow patterns, and may increase hydraulic gradients between groundwater and adjacent surface water systems. Although there are no direct discharge points to the receiving environment, indirect pollution pathways may still occur through runoff from disturbed mining areas, seepage from pollution control facilities, and episodic overflow events during periods of high rainfall.

2.2. Study Design

This study employed a quantitative research method, using historical physicochemical water quality data collected over a period of six years (from 2018 to 2023). The dataset comprises monthly monitoring data of five surface water monitoring points within the Leeuwfonteinspruit and its unnamed tributaries, both upstream and downstream of the active coal mining activities. The monitoring network included one site on the main Leeuwfonteinspruit upstream of the mining area (Site 1), one downstream site (Site 5), and three tributary sites (Sites 2–4) that drain into the Leeuwfonteinspruit between the upstream and downstream monitoring locations. This configuration enabled assessment of both tributary inputs and cumulative downstream water quality conditions. Figure 2 displays the monitoring locations, while Table 1 provides descriptions of the sampling sites in relation to mining area boundary, along with their geographical coordinates.

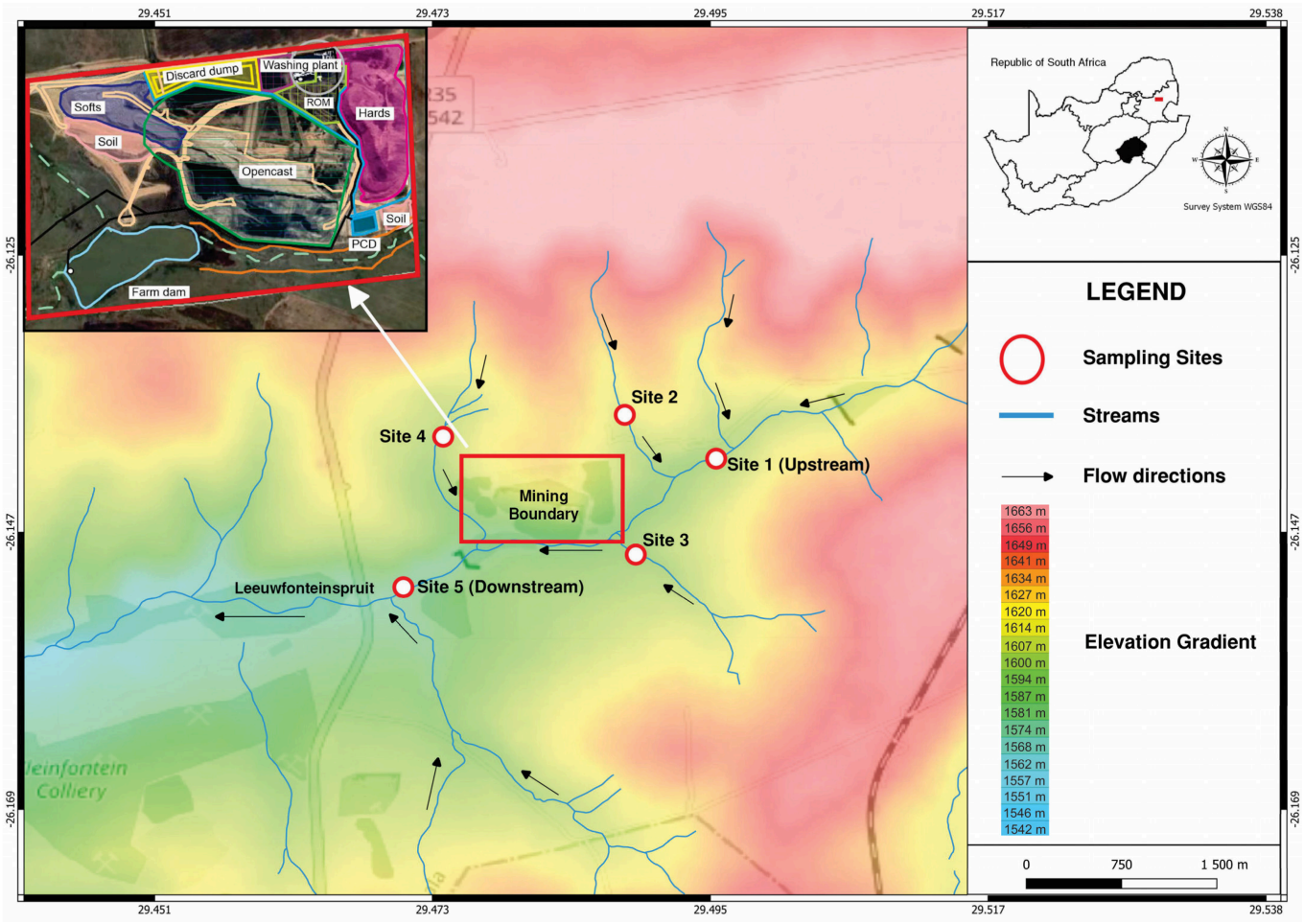


Figure 2. Surface water monitoring sites along Leeuwfonteinspruit. The map was prepared using QGIS Desktop (version 3.20.0). The study area was digitized using Google Earth Pro (version 7.3. The topographic background was derived from OpenStreetMap data and NASA Shuttle Radar Topography Mission elevation data.

Table 1. Monitoring localities and geographical coordinates.

Site	Co-Ordinates		Description
	Latitude	Longitude	
Site 1	26°08′26.03″ S	29°29′46.85″ E	Located upstream of the mining area in Leeuwfonteinspruit.
Site 2	26°08′16.00″ S	29°29′16.69″ E	Located upstream of the mining area (north-east) in a non-perennial stream of the Leeuwfonteinspruit.
Site 3	26°08′54.67″ S	29°29′18.78″ E	Located upstream of the mining area (southeast) in a non-perennial stream of the Leeuwfonteinspruit.
Site 4	26°08′21.39″ S	29°28′24.83″ E	Located upstream of the mining area (northern site) in a non-perennial stream of the Leeuwfonteinspruit.
Site 5	26°09′6.64″ S	29°28′11.68″ E	Located downstream of the mining area in the Leeuwfonteinspruit.

2.3. Field Data Collection

Surface water samples were collected monthly using the grab sampling method at monitoring localities indicated in Figure 2. At each site, in-field observations were recorded, including the visual characteristics of the water (unusual water color, the presence of algae, or any signs of contamination) and surrounding environmental conditions that can affect

the quality of the water. The sampling date and time were documented to establish a temporal context for the data. Weather conditions at the time of sampling were also noted, as they can significantly influence water quality parameters.

Each sample was assigned a unique identifier (sample name) to ensure traceability throughout the analytical process. Sampling locations were recorded using a handheld GPS device to ensure spatial accuracy, and photographic records were taken at each site to provide visual reference and support future comparative assessments.

Water samples were collected using clean 1-liter sampling bottles supplied by the laboratory. During sampling, bottles were submerged just below the water surface to minimize disturbance and avoid collection of surface debris. Bottles were filled completely and immediately sealed after collection.

Following collection, samples were stored in a cooler box with ice packs to maintain low temperatures and preserve sample integrity. All samples were transported to the laboratory on the same day of collection to minimize potential changes in physicochemical properties prior to analysis.

On-site measurements of selected physicochemical parameters, including pH, EC, and TDS, were conducted in situ using calibrated portable instruments.

2.4. Chemical Analysis of the Samples

Collected water samples were submitted to SANAS accredited laboratory (Regen Water (Pty) Ltd. laboratory in Witbank, South Africa) for the chemical analyses of the following elements: suspended solids (SS), nitrate and nitrite as N, chloride (Cl), total hardness as $CaCO_3$, total alkalinity as $CaCO_3$, potassium (K), fluoride (F), turbidity, phosphate (PO_4), SO_4, Na, Fe, Ca, Mg, Mn, and Al. All the laboratory analyses were performed according to the South African Bureau of Standards.

The SS were quantified through gravimetric analysis, which involved heating samples to 103–105 °C to evaporate water and determine the solid residue mass. For elemental analysis, including Mg, Ca, Na, K, Mn, Fe, and Al, Inductively Coupled Plasma—Optical Emission Spectrometry (Agilent 5110 ICP-OES; Agilent Technologies, Santa Clara, CA, USA) and Inductively Coupled Plasma—Mass Spectrometry (Agilent 7900 ICP-MS; Agilent Technologies, Santa Clara, CA, USA) methodologies were utilized, offering high sensitivity and specificity in detecting trace metals. Additionally, SO_4, Cl, and F concentrations were determined via Flow Injection Analysis, ensuring rapid and accurate results for these key ions. Total alkalinity and total hardness were measured using either automated or manual titration methods.

2.5. Quality Assurance and Quality Control

Quality assurance and quality control procedures were implemented throughout the sampling, analytical, and data management processes to ensure the reliability of the water quality dataset. Surface water samples were collected in sterilized laboratory-supplied polyethylene bottles and immediately stored in cooler boxes containing ice packs following collection. Samples were transported to the laboratory on the day of collection and submitted under chain-of-custody procedures to maintain sample traceability.

Field measurements of pH, EC, and TDS were conducted using calibrated instruments, with calibration performed prior to each monitoring event using appropriate standard solutions. Chemical analyses were undertaken by a SANAS-accredited laboratory (Regen Water (Pty) Ltd.) using approved analytical methods. Samples analyzed for dissolved metals were filtered prior to analysis and preserved with nitric acid or hydrochloric acid in accordance with laboratory procedures. Major cations (Ca, Mg, Na, K, Fe, Mn and Al) were

analyzed using ICP-OES and ICP-MS techniques, while nutrients and major anions were analyzed using discrete analyzer methods.

The laboratory maintained rigorous internal quality control procedures, including routine instrument calibration, quality control samples analyzed at regular intervals, certified reference materials, method validation, and participation in external proficiency testing programs. Quality control samples were analyzed after every 15 samples for ICP-OES, ICP-MS and nutrient analyses to verify instrument performance and analytical accuracy.

Minimum reporting limits were 0.1 mg/L for nitrate and nitrite, 1 mg/L for sulfate and chloride, 0.05 mg/L for calcium, sodium and potassium, 0.01 mg/L for magnesium and iron, 2 mg/L for suspended solids, and 0.2 NTU for turbidity. Following receipt of laboratory results, all data was verified against the original analytical certificates prior to statistical analysis. Quality checks were undertaken to identify transcription errors, inconsistencies, and incomplete records prior to data analysis.

As this study utilized historical monitoring data generated under an operational monitoring program, records of field blanks and duplicate samples were not consistently available for all sampling events and could therefore not be evaluated retrospectively.

2.6. Data Analysis

2.6.1. Water Quality Analysis

Water quality analysis provides a comprehensive assessment of the water within the coal mines, offering insights into areas of concern, the most detrimental parameters, the primary contaminants, and the sources of contamination [6]. By monitoring the physical and chemical aspects, it provides data on the presence of substances and their concentrations [29]. This monitoring aids in identifying the most effective methods for reducing water resource pollution and implementing appropriate measures to prevent contamination and serves as a preliminary alert mechanism to support effective and efficient planning [18]. Assessing water quality in coal mining is particularly important for human health and water resource management [42,43].

The water quality data was assessed against the SAWQGs developed by the Department of Water Affairs and Forestry (DWAF), now known as the Department of Water and Sanitation (DWS). The SAWQGs provide essential guidance for evaluating the suitability of water for various uses and supporting water quality management decisions. A key component of these guidelines is the Target Water Quality Range (TWQR), which defines the acceptable concentration range of specific constituents to ensure water remains fit for its intended use, even with long-term continuous exposure. In addition to safeguarding human uses, the TWQR also protects aquatic ecosystems [44].

In determining the appropriate guidelines for comparison, potential downstream users were identified through a review of aerial photographs, literature, and site visit observations. The evaluation of downstream users of the Leeuwfonteinspruit up to its confluence with the Olifants River included several usage classes: domestic users who use the water for washing and other domestic activities, aquatic species, irrigation users, and livestock watering. Therefore, the water quality was compared against the following guidelines:

- SAWQG Volume 1: Domestic Water Use [44].
- SAWQG Volume 4: Agricultural Water Use—Irrigation [45].
- SAWQG Volume 5: Agricultural Water Use—Livestock Watering [46].
- SAWQG Volume 7: Aquatic Ecosystem [47].

2.6.2. Water Quality Indices

The WQI is a mathematical approach that combines diverse factors, primarily physical and chemical, to evaluate the condition of surface water, groundwater, and lake water [33]. It synthesizes the collective effects of multiple water quality parameters, facilitating easy interpretation and utilization by water managers [48]. WQIs were computed to provide an overall assessment of water quality at each sampling site. These indices integrate multiple parameters into a single value, making it easy to compare water quality across different locations and identify areas of concern [18,33,35]. This study employed both the WA-WQI and CCME-WQI as complementary assessment tools, with the WA-WQI providing a weighted, parameter-based assessment and the CCME-WQI assessing compliance with the guideline limits, together strengthening the overall water quality assessment.

The Weighted Arithmetic Water Quality Index

The WA-WQI was computed using the weighted arithmetic index method, based on the class 1 drinking water quality standards set by the South African Bureau of Standards [31]. The WA-WQI method was adopted due to its ability to produce reliable results using a smaller set of water quality parameters. The method categorizes water quality into five classes based on WQI scores ranging from 0 to over 100 [28]. In this study, the following classification was used: excellent (0–25), good (26–50), poor (51–75), very poor (76–100), and unsuitable for use (>100). The mathematical formula of the WA-WQI is presented below:

We determine the unit weight, W_i, of each parameter using the equation below:

$$W_i = \frac{K}{S_i} \tag{1}$$

where K (constant of proportionality) is given by:

$$K = 1/\sum_{i=1}^{n} 1/S_i \tag{2}$$

S_i = Standard permissible value of the ith parameter.

The Sub-Index (Q_i) value was calculated by using the following equation:

$$Q_i = \frac{C_i - V_0}{S_i - V_0} \times 100 \tag{3}$$

where:

C_i = measured concentration of the ith parameters;

V_0 = Ideal value of the parameters in pure water (generally zero for most parameters and 7 for pH).

Finally, the WA-WQI was computed as:

$$WA - WQI = \frac{\sum_{i=1}^{n} (W_i \times Q_i)}{\sum_{i=1}^{n} W_i} \tag{4}$$

Canadian Council of Ministers of the Environment Water Quality Index

The application of the CCME-WQI has been on the rise in assessing the pollution of water. This index efficiently consolidates various sets of biological, chemical, and physical data pertaining to water quality into a singular metric, indicating contamination levels [33]. The CCME-WQI provides a practical approach to simplify complex water quality data, making it more accessible for communication to a wide audience [35]. Table 2 presents the water quality classifications based on the CCME-WQI.

Table 2. CCME-WQI rankings for the water quality classifications.

Water Quality Index Level	Water Quality Rank
0–44	Poor
45–64	Marginal
65–79	Fair
80–94	Good
95–100	Excellent

The mathematical formula of the CCME-WQI is presented below:

$$CCME - WQI = 100 - \frac{\sqrt{F_1{}^2 + F_2{}^2 + F_3{}^2}}{1.732} \quad (5)$$

F_1 (scope) represents the percentage of variables that deviate from their objectives at least once, relative to the total number of variables measured.

$$F_1 = \frac{number\ of\ failed\ variables}{total\ number\ of\ variables} \times 100 \quad (6)$$

F_2 (frequency) represents the percentage of individual tests that fail to meet their objectives.

$$F_2 = \frac{number\ of\ failed\ tests}{total\ number\ of\ tests} \times 100 \quad (7)$$

F_3 (amplitude) is an asymptotic capping function that adjusts the normalized sum of the excursions from objectives (nse), ensuring the results fall within a range of 0 to 100.

$$F_3 = \frac{nse}{0.01nse + 0.01} \quad (8)$$

where:

$$nse = \frac{\sum_{i=1}^{n} Excursion_i}{Number\ of\ tests} \quad (9)$$

For instances where the test value must not exceed the objective:

$$Excursion_i = \frac{Failed\ Test_i}{Objective_j} - 1 \quad (10)$$

For instances where the test value must not fall below the objective:

$$Excursion_i = \frac{Objective_j}{Failed\ Test_i} - 1 \quad (11)$$

For instances where the objective is zero:

$$Excursion_i = Failed\ Test_i \quad (12)$$

2.6.3. Water Quality Suitability for Irrigation

Sodium Adsorption Ratio (SAR)

The SAR is essential for determining the suitability of surface water for irrigation. High SAR values can negatively affect soil structure by reducing hydraulic conductivity [28,49]. Based on SAR, water is classified as excellent (<10), good (10–18), doubtful (18–26), and unsuitable (>26).

Prior to calculating the SAR, the concentrations of Na^+, Ca^{2+}, and Mg^{2+} were converted from milligrams per liter (mg/L) to milliequivalents per liter (meq/L) using their respective equivalent weights. The conversion was performed according to the equation below:

$$meq/L = \frac{Concentration\ (mg/L)}{Equivalent\ Weight} \quad (13)$$

where Equivalent Weight is calculated using the following equation:

$$Equivalent\ Weight = \frac{Atomic\ mass}{Ionic\ valence} \quad (14)$$

The converted concentrations were subsequently used to calculate the SAR using the following equation:

$$SAR = \frac{Na^+}{\sqrt{\frac{Mg^{2+}+Ca^{2+}}{2}}} \quad (15)$$

Sodium percentage (Na%)

The Na% is a widely used irrigation water quality index that evaluates the relative abundance of Na^+ in water. Elevated Na concentrations in irrigation water can adversely affect both soil properties and crop productivity. Excess Na tends to be adsorbed onto soil cation exchange sites, displacing Ca and Mg and causing the breakdown of soil aggregates. This process reduces soil permeability, restricts water infiltration and aeration, and ultimately impairs the soil's ability to support healthy plant growth [28,32]. The Na% categorizes water as excellent (<20%), good (20–40%), permissible (40–60%), doubtful (60–80%), and unsuitable (>80%) for irrigation purposes. Na% was calculated using the equation below:

$$Na\% = \frac{Na^+}{Ca^{2+} + Mg^{2+} + Na^+ + K^+} \times 100 \quad (16)$$

The calculation of Na% was based on ionic concentrations expressed in meq/L, using the same conversion procedure described in Equations (14) and (15).

United States Salinity Laboratory (USSL) diagram

The irrigation suitability of the surface water was further evaluated using the USSL diagram [50]. The USSL diagram classifies irrigation water according to its salinity hazard, represented by EC, and sodicity hazard, represented by the SAR. Prior to plotting, EC values were converted from mS/m to µS/cm to conform to the standard USSL classification system. The resulting plot was used to classify the water samples into salinity hazard classes ranging from C1 (low salinity) to C4 (very high salinity) and sodium hazard classes ranging from S1 (low sodium hazard) to S4 (very high sodium hazard), thereby providing an integrated assessment of irrigation suitability. Water samples within the higher salinity (C3–C4) and sodium hazard (S3–S4) classes indicate increasing restrictions for irrigation use, whereas those within the lower hazard classes (C1–C2 and S1–S2) are generally considered suitable for irrigation under appropriate management practices [50].

2.6.4. Gibbs Diagram Analysis

The Gibbs diagram is a hydrogeochemical tool used to identify the dominant natural processes controlling the evolution of water quality [51]. It helps to interpret environmental processes such as dilution, evaporation–concentration, mineral dissolution, mixing, and the influence of water residence time within the reservoir. In this study, Gibbs diagrams were constructed by plotting TDS against the ratio of Na to the sum of Na and Ca for cations, and the ratio of Cl to the sum of Cl and SO_4 for anions [31,52].

This approach enables the determination of the prevailing geochemical control field by relating the cation and anion dominance against TDS concentrations. The three possible control fields are:

- Precipitation dominance—characterized by low TDS values against minimal SO_4 and Ca concentrations.
- Rock dominance—associated with moderate TDS and water chemistry influenced by the dissolution of silicate and carbonate rocks.
- Evaporation–crystallization dominance—defined by high TDS and elevated ion concentrations due to evaporation or poor drainage.

2.6.5. Sequential Mann–Kendall

The SMK test was performed using R (version 4.4.2) to evaluate temporal trends and identify potential change points in the WA-WQI, SAR, and Na% across the monitoring sites. The SMK test is a non-parametric extension of the conventional Mann–Kendall test that enables the detection of not only the direction and significance of monotonic trends but also the approximate timing of trend initiation and abrupt changes within a time series [31,53,54].

The SMK is computed using the ranked values, y_i of the original observations $(x_1, x_2, x_3, \ldots, x_n)$, each value of $y_i (i = 1, 2, 3, \ldots, n)$ is sequentially compared with all preceding values y_j, where $j = 1, 2, 3, \ldots, i-1$. During each comparison, a count n_i is assigned whenever $y_i > y_j$, and the cumulative sum of these counts is used to calculate the statistic t_i. The statistic t_i is subsequently employed to determine the expected value, $E(t_i)$, and the variance, $Var(t_i)$, of the test statistic, as presented in the following equations:

$$t_i = \sum_{k=1}^{i} n_k \tag{17}$$

$$E(t_i) = \frac{i(i-1)}{4} \tag{18}$$

$$Var(t_i) = \frac{i(i-1)(2i+5)}{72} \tag{19}$$

The standardized progressive statistic $(u(t)_i)$ is then computed as:

$$u(t_i) = \frac{[t_i - E(t_i)]}{\sqrt{VAR(t_i)}} \tag{20}$$

Similarly, the retrogressive sequence $u'(t_i)$ is computed by applying the same procedure to the reversed time series, beginning with the final observation and proceeding backwards to the first observation [54,55]. The $u'(t_i)$ values are subsequently rearranged in chronological order and plotted together with the $u(t)_i$ series.

Positive $u(t)_i$ values indicate increasing trends, whereas negative values indicate decreasing trends. The significance of the trends was evaluated using the 95% confidence limits (± 1.96). Values of $u(t)_i$ exceeding +1.96 indicate statistically significant increasing trends, while values below -1.96 indicate statistically significant decreasing trends. The intersection of the progressive and retrogressive curves identifies the approximate timing of a potential turning point or abrupt change in the temporal behavior of the dataset. Intersections occurring within the confidence boundaries are considered indicative of significant change points, whereas intersections outside these limits suggest possible but statistically insignificant changes [54,55].

One limitation of the SMK test is that it does not explicitly account for seasonality and serial autocorrelation, both of which may influence monthly water quality datasets. Con-

sequently, the identified trends should be interpreted as indicative of long-term temporal patterns and potential change points rather than precise estimates of trend magnitude.

2.6.6. Statistical Analysis

The water quality data was analyzed by calculating the mean, median, standard deviation, and range for each parameter using Microsoft Excel. This approach provided an overview of the data distribution, highlighting central tendencies and variability, and helped identify any anomalies in the dataset. Microsoft Excel was also used to conduct temporal trend analysis for WA-WQI, SAR, and Na% for each monitoring point.

The IBM SPSS (version 30.0), a commercial statistical software program, was used to perform multivariate statistical analysis, such as PCA, to determine potential sources of contamination affecting Leeuwfonteinspruit. PCA reduced the dataset's dimensionality, revealed patterns among water quality parameters, and identified underlying factors representing the possible pollution sources [33,37]. Additionally, correlation analysis was used to determine the level of association between the key water quality parameters [36].

3. Results and Discussion

3.1. Water Chemistry

The annual average water quality results from 2018 to 2023 for the selected parameters are presented in Table 3. The values presented are based on the varying sample sizes, where Sites 1, 2, 3, and 5 were sampled monthly throughout the study period (n = 72 per site), while Site 4 experienced seasonal dry conditions, resulting in variable sampling frequencies per year (2018: n = 5; 2019: n = 3; 2020: n = 9; 2021: n = 9; 2022: n = 12; 2023: n = 11).

Table 3. Annual average water quality results for selected parameters from 2018 to 2023.

Chemical Variables		TDS (mg/L)	SO_4 (mg/L)	Ca (mg/L)	Mg (mg/L)	Na (mg/L)	Fe (mg/L)	Mn (mg/L)	EC (mS/m)	pH	Al (mg/L)
TWQR	Domestic use	450	200	32	30	100	0.10	0.05	70	6.0–9.0	0.15
	Aquatic Ecosystem	NA	NA	NA	NA	NA	NA	0.18	NA	NA	0.01
	Agricultural: Irrigation	260	NA	NA	NA	70	5	0.02	40	6.5–8.4	5
	Agricultural: Livestock	1000	1000	1000	500	2000	10	10	150	NA	5
2018	Site 1	296.00	40.30	23.18	16.36	49.16	0.45	0.02	49.54	8.16	0.08
	Site 2	486.33	108.48	47.04	26.99	72.87	0.20	0.17	75.75	7.77	0.14
	Site 3	445.83	23.89	46.44	24.03	74.76	2.65	2.52	72.98	7.62	0.46
	Site 4	182.50	57.31	30.83	8.02	12.71	0.22	0.03	28.18	6.77	0.24
	Site 5	249.00	65.15	28.91	13.54	33.03	0.10	0.01	40.43	7.45	0.09
2019	Site 1	294.67	59.18	27.19	16.94	41.07	0.40	0.04	47.28	8.06	0.49
	Site 2	355.50	77.52	42.45	19.69	48.76	0.43	0.63	56.47	7.53	0.30
	Site 3	421.17	69.07	45.33	24.14	57.02	1.02	0.91	65.86	7.36	0.14
	Site 4	196.00	89.00	16.60	6.73	19.35	4.93	0.67	24.55	6.76	2.65
	Site 5	369.00	137.58	38.58	18.98	41.45	0.77	0.06	54.79	7.36	1.06
2020	Site 1	277.17	55.99	22.02	14.78	44.20	0.24	0.02	44.44	8.00	0.11
	Site 2	584.17	144.49	61.22	34.48	72.62	0.70	2.95	86.89	7.86	0.43
	Site 3	377.50	52.19	38.89	21.02	62.20	0.49	0.32	60.82	7.62	0.92
	Site 4	204.00	89.31	20.24	7.49	19.98	1.08	0.20	25.45	6.82	2.34
	Site 5	477.83	234.58	46.97	21.83	60.65	0.22	0.06	67.98	7.75	0.29

Table 3. *Cont.*

Chemical Variables		TDS (mg/L)	SO_4 (mg/L)	Ca (mg/L)	Mg (mg/L)	Na (mg/L)	Fe (mg/L)	Mn (mg/L)	EC (mS/m)	pH	Al (mg/L)
2021	Site 1	310.67	64.76	22.23	16.59	51.89	0.20	0.01	50.28	8.31	0.10
	Site 2	441.83	104.84	45.01	26.04	64.88	0.25	0.06	71.34	7.83	0.31
	Site 3	495.50	58.84	49.52	33.05	68.72	0.67	0.34	77.62	7.84	0.25
	Site 4	222.50	71.90	25.25	10.31	12.22	4.53	1.19	32.38	6.98	0.48
	Site 5	674.00	366.00	70.96	33.93	82.82	0.10	0.03	94.28	7.88	0.08
2022	Site 1	238.83	26.05	22.50	14.32	30.43	0.13	0.02	37.28	7.68	0.08
	Site 2	355.17	75.04	39.84	20.79	42.20	0.41	0.07	55.51	7.54	0.28
	Site 3	285.17	26.61	29.28	14.01	39.46	1.30	0.47	42.67	7.44	0.38
	Site 4	311.00	83.83	32.04	14.82	34.19	1.30	0.54	45.08	7.07	1.02
	Site 5	467.17	188.36	53.25	28.75	49.53	0.39	0.19	66.66	7.27	0.16
2023	Site 1	285.50	37.23	26.87	18.82	38.27	0.17	1.09	45.98	7.59	0.06
	Site 2	412.00	86.86	42.93	24.59	55.96	0.34	0.16	64.91	7.59	0.39
	Site 3	322.33	32.17	36.61	20.05	43.86	0.42	0.29	53.19	7.34	0.08
	Site 4	503.27	159.90	51.57	25.08	65.88	0.16	1.74	73.16	7.20	0.15
	Site 5	690.50	360.30	77.78	39.00	72.92	0.13	0.03	95.21	7.51	0.08

The annual average water quality results were assessed against the applicable SAWQGs as developed by DWAF. This section focuses on parameters that either exceed the TWQR limits on more than two occasions during the monitoring period or are recognized in the literature as key indicators of coal mining impacts on surface water quality.

The TDS concentrations ranged from 182.50 mg/L to a maximum of 690.50 mg/L. The upstream sites (Sites 1–4) generally exhibited lower TDS concentrations than the downstream site (Site 5). While elevated TDS concentrations were also observed at some upstream sites, Site 5 recorded the highest concentrations during the latter years of the study (2021–2023). Notably, TDS at Site 5 increased from 249.00 mg/L in 2018 to 690.50 mg/L in 2023, indicating a progressive accumulation of dissolved solids that is likely associated with the cumulative influence of upstream mining and other catchment activities.

Most TDS concentrations complied with the TWQR for domestic use of 450 mg/L [44]. However, exceedances were recorded at Site 2 (2018 and 2020), Site 3 (2021), Site 4 (2023), and Site 5 (2020, 2021, 2022, and 2023). All measured TDS concentrations remained below the livestock watering guideline of 1 000 mg/L [46], indicating that the water was generally suitable for livestock use. In contrast, the irrigation guideline of 260 mg/L DWAF [45] was exceeded at most monitoring sites for much of the study period, indicating that salinity may pose a constraint for the irrigation of salt-sensitive crops. Exceedances were widespread across the catchment, with the greatest frequency and persistence occurring at Sites 1, 2, 3, and the downstream Site 5, while Site 4 only exceeded the guideline during the latter part of the monitoring period (2022 and 2023). These findings suggest progressive salinity enrichment associated with the catchment activities.

Electrical Conductivity (EC), which reflects TDS and overall water salinity, varied from 24.55 mS/m to a peak of 95.21 mS/m. The EC trends closely mirrored the TDS trends, with a significant increase observed at Site 4 (from 28.18 mS/m in 2018 to 95.21 mS/m in 2023). The increasing EC levels indicate a gradual accumulation of dissolved ions over time, potentially linked to ongoing mining activities in the catchment [35]. The EC concentrations exceeded DWAF's (1996a) TWQR for domestic use (70 mS/m) at various sites and years, notably at Site 2 and Site 3 in 2018; Site 2, Site 3, and Site 5 in 2021; Site 4 and Site 5 in 2023. For irrigation purposes, with a limit of 40 mS/m [45], EC values were consistently above the limit across most sites, except at Site 4 between 2018 and 2021, and Site 1 in 2022. Despite these exceedances, all EC concentrations remained within the limit for livestock watering (150 mS/m) throughout the monitoring period [46].

The pH values remained relatively stable across all the monitoring sites and generally reflected neutral water conditions. Measurements ranged from 6.76 to 8.31 and were consistently within the DWAF TWQR for both domestic use and irrigation [44,45]. Site 4 recorded the lowest pH values, suggesting a greater susceptibility to acidification. Despite elevated SO_4 concentrations, Site 5 maintained neutral pH levels (7.27–7.88), likely due to natural buffering mechanisms. These results align with studies showing that alkaline minerals can buffer acidity and maintain neutral pH [17,39,56].

The SO_4 concentrations ranged from 23.89 mg/L to a peak of 366 mg/L. Upstream sites indicated lower SO_4 concentrations and were all within the TWQR for domestic use with a limit of 200 mg/L [44]. However, exceedances at the downstream site (Site 5) were recorded in 2020, 2021, and 2023, indicating potential influence from mine-related inputs. Despite these exceedances, all values complied with the TWQR for livestock watering with a limit of 1000 mg/L [46].

On the other hand, Ca concentrations ranged from 16.6 to 77.78 mg/L, with frequent exceedances of the TWQR for domestic use with a limit of 32 mg/L [44]. Elevated Ca levels were notable at Sites 2, 3, and 5, while Site 1 consistently recorded lower, compliant values. Site 5 indicated an increasing trend over the monitoring period, from 28.91 mg/L to 77.78 mg/L in 2023. Despite the exceedances for domestic use, all sites remained well within the TWQR for livestock watering with a limit of 1000 mg/L [46].

With Mg, the levels ranged from 6.73 mg/L to 39.00 mg/L, with several sites exceeding the TWQR for domestic use with a limit of 30 mg/L [44], including Site 2 (2020), Site 3 (2021), and Site 5 (2021 and 2023). However, all sites remained compliant with the TWQR for livestock watering, which has a limit of 500 mg/L [46].

While Na levels were generally within the domestic use limit of 100 mg/L DWAF [44] at all the sites throughout the monitoring period. However, exceedances of DWAF (1996b) TWQR for irrigation with a limit of 70 mg/L were noted at Site 2 in 2018 and 2020, Site 3 in 2018, and Site 5 in both 2021 and 2023. Despite these occasional exceedances, all sites remained within the acceptable TWQR for livestock watering with a limit of 2000 mg/L [46].

For metals such as Fe, Al and Mn, variations in the concentrations were also observed at the different sites. The levels of Fe consistently exceeded the DWAF (1996a) TWQR for domestic use (0.1 mg/L) across all sites and years, except for Site 5 in 2018 and 2021. The highest Fe concentrations were recorded at Site 4 in 2019 (4.93 mg/L) and 2021 (4.53 mg/L). However, all sites remained within acceptable limits for irrigation (5 mg/L) and livestock watering (10 mg/L) throughout the entire study period [45,46].

The concentrations of Mn indicated significant variability across monitoring sites, with the highest levels recorded at Site 3 in 2018 (2.52 mg/L) and Site 2 in 2020 (2.95 mg/L). Most sites consistently exceeded both the TWQR for domestic use (0.05 mg/L) and the irrigation limit of 0.02 mg/L [44,45]. Notable exceptions to irrigation exceedances included Site 1 in 2018, 2020, 2021, and 2022, as well as Site 5 in 2018. Mn levels regularly exceeded the aquatic ecosystem guideline of 0.18 mg/L [47], with Site 3 consistently above the limit throughout the monitoring period and Site 4 exceeding the limit in all the years except for 2018. Despite these exceedances, all sites remained well within the TWQR for livestock watering with a limit of 10 mg/L [46].

The Al concentrations consistently exceeded the TWQRs for domestic use (0.15 mg/L) and aquatic ecosystem (0.05 mg/L) across all monitoring sites and years [44,47]. However, all sites remained within the acceptable limits for both irrigation and livestock watering (5 mg/L) throughout the entire period [45,46].

3.2. Water Quality Indices

Weighted arithmetic water quality index

The WA-WQI was computed to evaluate the overall water quality status in the Leeuwfonteinspruit across five sites. The distribution of WA-WQI values is presented in Figure 3 and Table 4. Across the 72 sampling events, WQI values ranged from 12.45 to >100, reflecting substantial temporal and spatial variability. The interquartile ranges varied across sites as follows: Site 1 (33–92), Site 2 (43 $\geq$ 100), Site 3 (47 $\geq$ 100), Site 4 (49 $\geq$ 100), and Site 5 (46 $\geq$ 100). These ranges indicate that most sites fluctuated between good to poor water quality classes, with episodic exceedances into severely degraded water quality (>100).

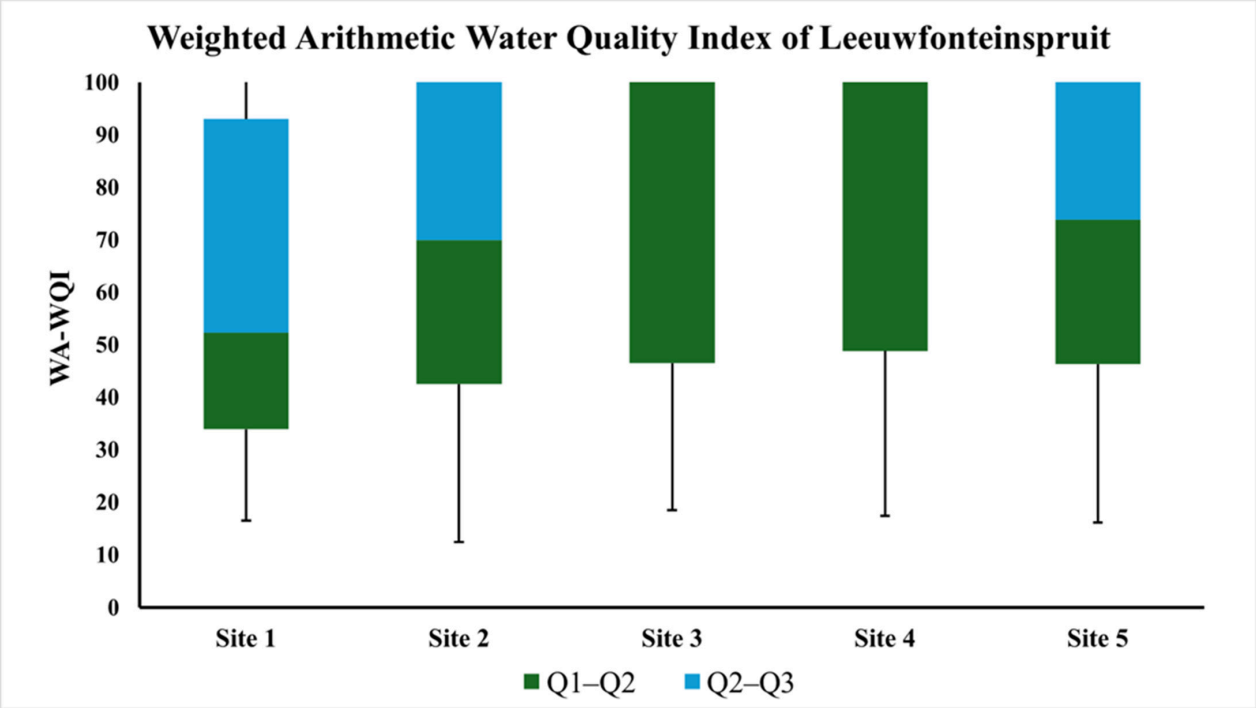


Figure 3. Boxplot distribution of WA-WQI values at five sites (Sites 1–5) within Leeuwfonteinspruit. The interquartile range (Q1–Q3) is visually divided into lower (Q1–Q2) and upper (Q2–Q3) segments for improved visual interpretation.

Table 4. Frequency distribution of WQI classes across monitoring sites in the Leeuwfonteinspruit.

WQI Class	Range	Site 1	Site 2	Site 3	Site 4	Site 5
Excellent	WQI $\leq$ 25	6	7	2	2	5
Good	26 $\leq$ WQI $\leq$ 50	27	14	20	9	14
Poor	51 $\leq$ WQI $\leq$ 75	18	18	9	6	19
Very Poor	76 $\leq$ WQI $\leq$ 100	3	5	5	2	14
Unsuitable for Use	WQI > 100	18	28	36	22	20

In terms of water quality classifications, Sites 1 and 2 recorded the highest frequency of excellent water quality, with six and seven samples, respectively, followed by Site 5 with five instances. In contrast, Sites 3 and 4 each recorded only two excellent water quality events. For the good water quality category, Site 1 stood out with 27 samples, indicating relatively stable and favorable conditions, possibly due to its upstream position and limited exposure to intensive pollution sources. In contrast, the downstream site (Site 5), recorded a combined total of 33 samples in the poor and very-poor categories, reflecting the cumulative impact of upstream pollution exacerbated by runoff or direct discharges from mining activities.

The most critical concern arises from the unsuitable for use category. Site 3 recorded the highest frequency of such events, despite being upstream, suggesting the presence of persistent pollution sources from the upper catchment. Similarly, Sites 2 and 4 also exhibited notable occurrences of unsuitable water quality, indicating that upstream areas of the catchment are also vulnerable to significant water degradation. Overall, Site 1 emerged as the least impacted, showing the most consistent good to excellent water quality. In contrast, Site 3 appeared the most vulnerable, reflecting persistent upstream pollution, while Site 5 presented a mixed water quality profile, characterized by both episodic improvements and cumulative degradation.

CCME-WQI assessment

The CCME-WQI was calculated to evaluate the annual surface water quality at five sites within the Leeuwfonteinspruit catchment. The annual CCME-WQI and corresponding ranking for each sampling site are presented in Table 5.

Table 5. Annual CCME-WQI scores and water quality rankings for sampling Sites 1–5 (2018–2023).

Year	Sampling Site	F1	F2	F3	CCME WQI	WQI Ranking
2018	Site 1	42.86	10.71	21.43	71.92	Fair
	Site 2	78.57	30.36	29.55	49.23	Marginal
	Site 3	71.43	30.36	84.98	34.07	Poor
	Site 4	28.57	21.43	16.99	79.83	Good
	Site 5	28.57	38.69	4.74	82.69	Good
2019	Site 1	50.00	17.26	30.34	64.79	Fair
	Site 2	64.29	24.40	55.15	49.11	Marginal
	Site 3	71.43	25.00	67.06	41.62	Poor
	Site 4	21.43	21.43	84.65	48.09	Marginal
	Site 5	71.43	25.60	51.79	46.96	Marginal
2020	Site 1	42.86	8.93	10.80	73.97	Fair
	Site 2	78.57	35.12	83.09	30.93	Poor
	Site 3	64.29	20.24	53.92	50.17	Marginal
	Site 4	21.43	14.29	66.67	58.74	Marginal
	Site 5	71.43	26.79	27.62	53.16	Marginal
2021	Site 1	57.14	10.71	8.33	66.09	Fair
	Site 2	78.57	30.36	23.61	49.49	Marginal
	Site 3	78.57	30.36	51.76	42.92	Poor
	Site 4	28.57	21.43	83.25	47.70	Marginal
	Site 5	64.29	38.69	19.66	55.22	Marginal
2022	Site 1	21.43	4.76	4.44	87.07	Good
	Site 2	42.86	20.24	28.01	68.22	Fair
	Site 3	35.71	13.69	60.88	58.49	Marginal
	Site 4	57.14	21.43	67.01	47.67	Marginal
	Site 5	64.29	30.95	36.81	53.65	Marginal
2023	Site 1	50.00	11.90	61.04	53.93	Marginal
	Site 2	71.43	24.40	35.95	51.73	Marginal
	Site 3	50.00	17.26	38.54	62.21	Marginal
	Site 4	78.57	31.82	72.62	35.55	Poor
	Site 5	57.14	31.55	25.07	59.63	Marginal

In 2018, water quality for Sites 4 and 5 was classified as good and Site 1 as fair. However, Sites 2 and 3 exhibited early signs of water quality degradation, with marginal to poor rankings. These early poor water qualities reflect the impacts of upstream anthropogenic activities, including mining and agricultural activities. Between 2019 and 2021, water quality degraded at all sites, with marginal and poor classifications becoming dominant. Notably, Site 3 ranked poor in both 2019 and 2021, while Site 2 never exceeded marginal quality within that period, indicating ongoing degradation.

A temporary improvement was observed in 2022, when Site 1 improved to good (WQI = 87.07) and Site 2 to fair (WQI = 68.2). This short-term improvement in water quality may have been influenced by improved management practices, favorable climatic conditions (e.g., dilution during high rainfall events), or seasonal hydrological variability. However, these improvements were not sustained, as most sites reverted to marginal in 2023, and Site 4 indicated a sharp decline to poor (WQI = 35.55).

Site 5 reflected the cumulative impact of upstream disturbances, consistent with mining-related inputs. Initially classified as good in 2018 (WQI = 82.69), indicating a relatively healthy catchment prior to intensified mining activities. However, subsequent years indicate consistently marginal water quality, with WQI ranging between 46.96 (2019) and 59.63 (2023). This degradation trend, especially after 2019, correlates with increased surface disturbances, runoff, and potential discharge events.

3.3. Water Quality Suitability for Irrigation

Sodium (Na) is a key parameter in assessing the irrigation water quality. Elevated Na levels can displace Ca and Mg, leading to soil structural deterioration, reduced permeability, and impede water and air movement, ultimately reducing crop productivity. Furthermore, interactions with carbonate and chloride can result in the development of alkaline or saline soils [32,57].

Sodium adsorption ratio

The SAR is used to determine the risk of Na accumulation in soils, which can displace Ca, Mg and K, thereby reducing water movement and prolonging percolation time [32].

Figure 4 presents the boxplot of SAR across the sites. Across all five sites in the Leeuwfonteinspruit, the SAR values consistently remained below 10, indicating that Na is not dominant relative to Ca and Mg, and the risk of sodicity-related soil degradation is currently minimal.

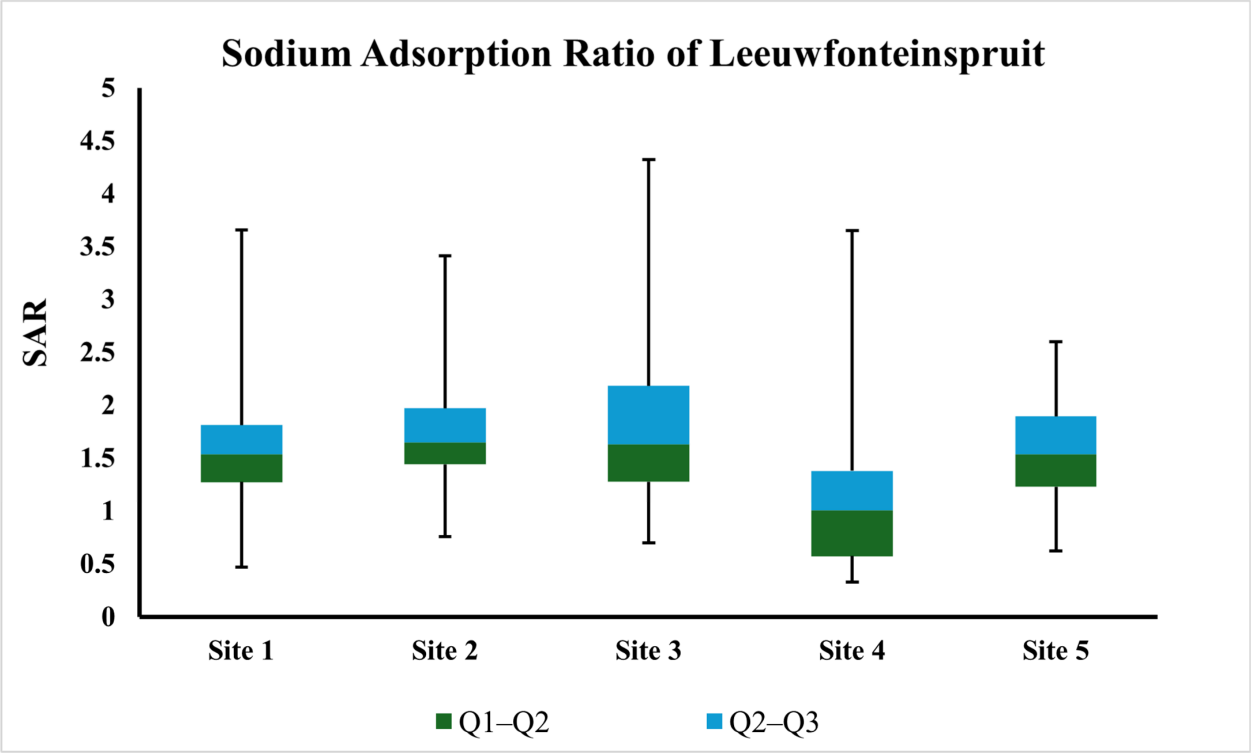


Figure 4. The distribution of SAR values at five sites within Leeuwfonteinspruit. The interquartile range (Q1–Q3) is visually divided into lower (Q1–Q2) and upper (Q2–Q3) segments for improved visual interpretation.

Site-specific differences were also observed. Sites 1 and 2 recorded median SAR values of 1.5 and 1.6, respectively, while occasional peaks approached 3.6 and 3.4. Site 3 exhibited the highest variability, with values exceeding 4.0 during certain periods, pointing to localized Na enrichment and increased susceptibility to sodicity, which can negatively affect the soil structure and plant growth. In contrast, Site 4 consistently recorded the lowest values (median 1.0), reflecting possible natural dilution. Downstream at Site 5, SAR values were intermediate (median of 1.5, maximum 2.6), indicating partial attenuation and recovery of Na impacts.

Sodium percentage

The Na% values across the five sites of the Leeuwfonteinspruit demonstrate both spatial and temporal variability over the monitoring period, with values ranging as low as 13% at Site 4 to as high as 66% at Site 3, as illustrated in the boxplot (Figure 5).

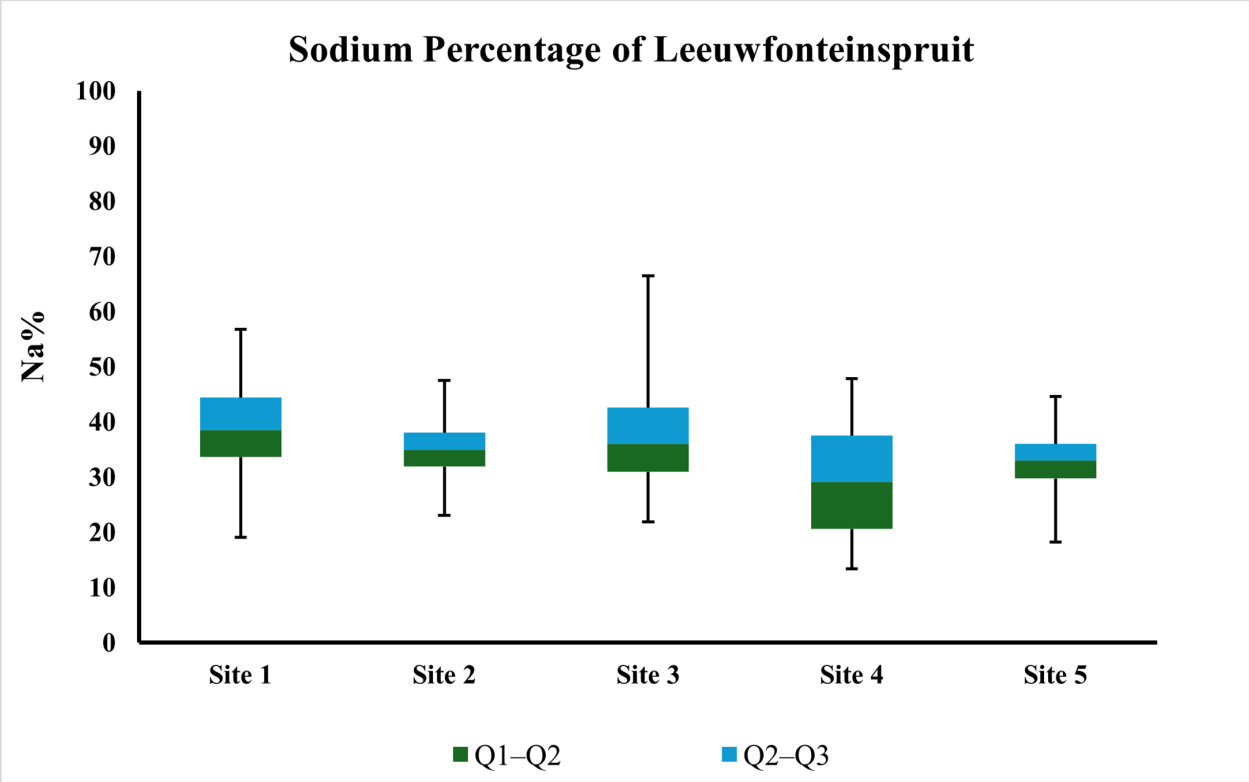


Figure 5. The distribution of Na% values at five sites within Leeuwfonteinspruit. The interquartile range (Q1–Q3) is visually divided into lower (Q1–Q2) and upper (Q2–Q3) segments for improved visual interpretation.

At Site 1, Na% values varied considerably (19–56%), with a median of 38% placing it mostly within the good category. However, recurrent peaks above 50% indicate periodic increases in Na dominance and a potential sodicity risk. Site 2 displayed a relatively narrow range (23–47%), with values predominantly within the good category, suggesting comparatively stable irrigation water quality throughout the monitoring period. Site 3 exhibited the greatest variability (22–66%) and recorded the highest maximum Na% value within the catchment. Although the median value of 36% remained within the good category, occasional values exceeding 60% indicate periods during which irrigation suitability deteriorated to the doubtful category. In contrast, Site 4 recorded the lowest Na% values (13–48%), with a median of 29% (good category). Downstream, Site 5 showed intermediate values (18–45%) with a median of 33%, predominantly within the good category, although occasional exceedances into the permissible category were observed.

Overall, the Na% analysis indicates that Na hazard remains generally low-to-moderate across the catchment, with most samples falling within the good category for irrigation. Although occasional increases in Na% were observed, particularly at Sites 1 and 3, these were infrequent and do not indicate a persistent sodicity hazard. The observed variability likely reflects the combined influence of natural hydrochemical processes and catchment activities.

Irrigation suitability based on the USSL diagram

The USSL diagram (Figure 6) indicates that all water samples fall within the S1 (low sodium hazard) class, demonstrating a minimal risk of soil sodicity. Most samples are classified within the C2–S1 and C3–S1 categories, representing medium to high salinity hazards coupled with low sodium hazards, whereas a smaller proportion of samples fall within the C1–S1 category, indicating low salinity and low sodium hazards. The predominance of the C2–S1 and C3–S1 classes indicates that irrigation suitability within the Leeuwfonteinspruit is primarily constrained by salinity rather than sodium accumulation. Consequently, although the water is generally suitable for irrigation with respect to sodicity, salinity management practices may be required where elevated salinity occurs. Overall, the USSL classification corroborates the EC, TDS, SAR, and Na% results, confirming that progressive salinity enrichment, rather than sodicity, represents the principal limitation for irrigation within the catchment.

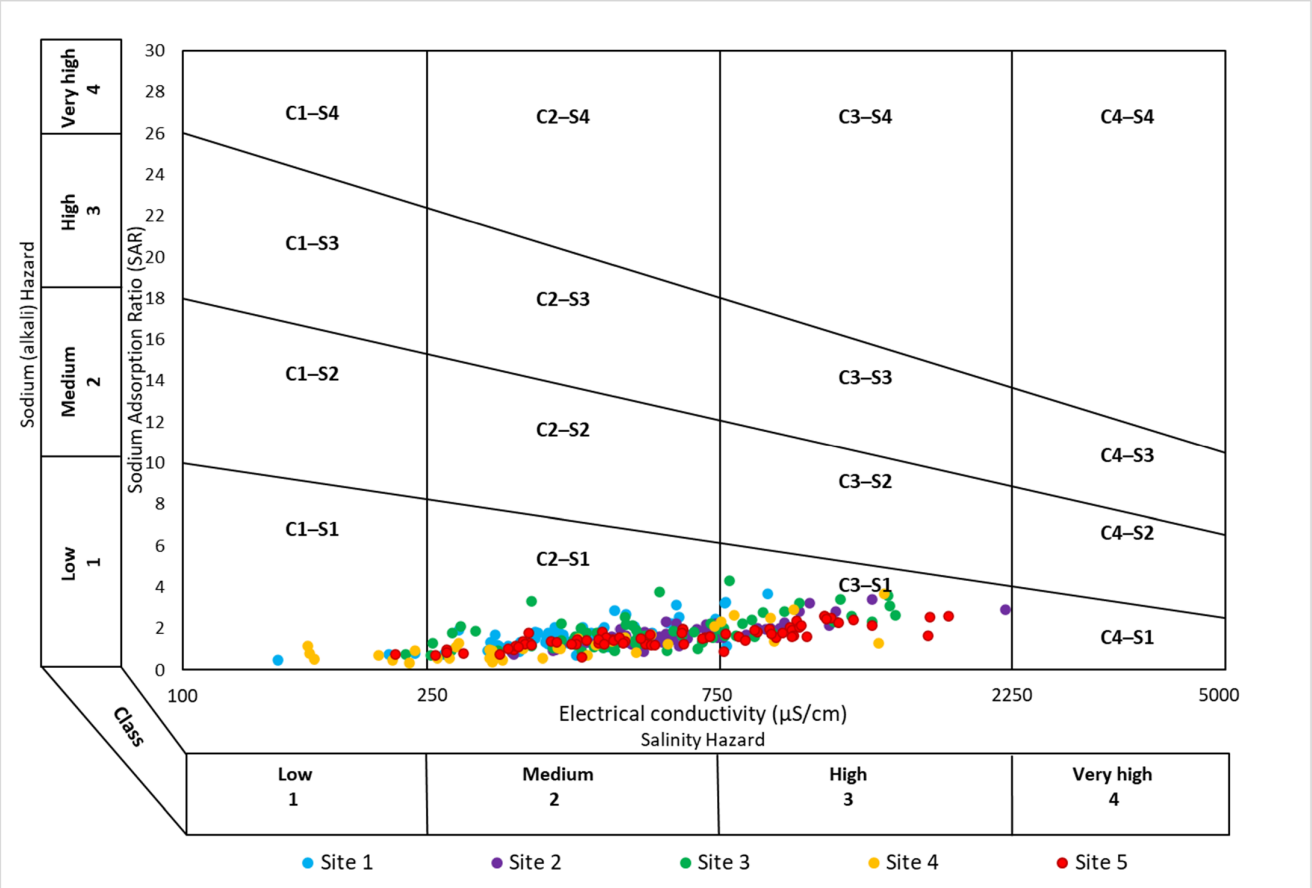
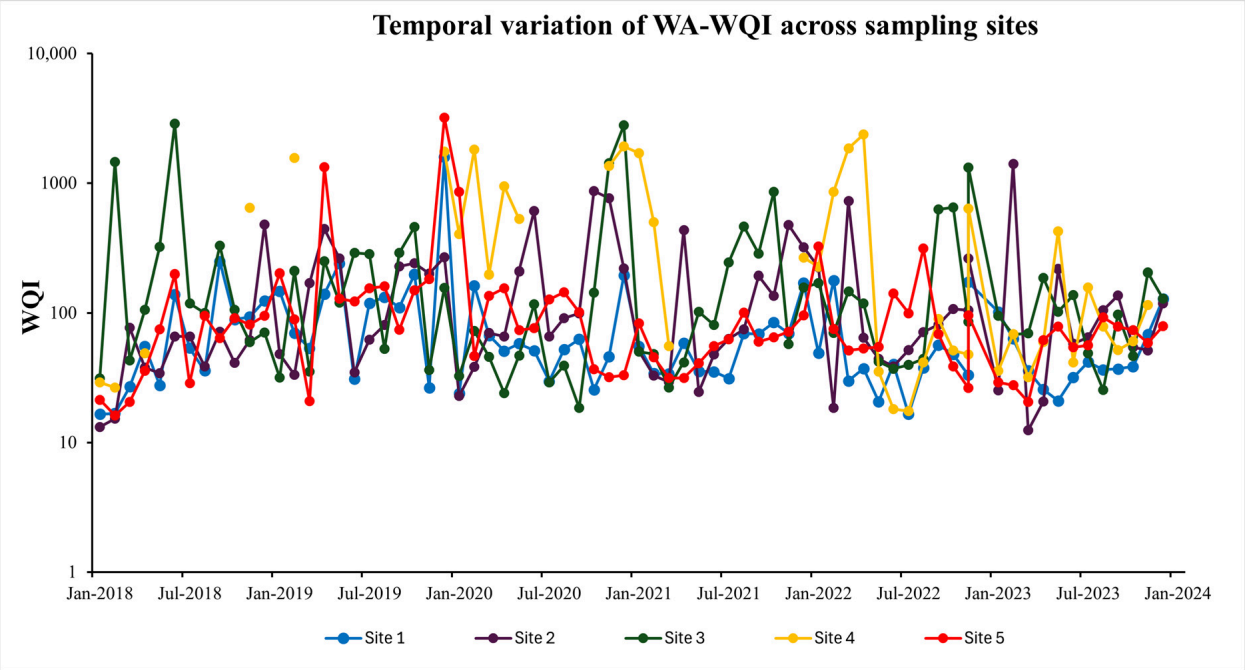


Figure 6. The USSL diagram showing the irrigation suitability of surface water samples from the Leeuwfonteinspruit based on EC and SAR.

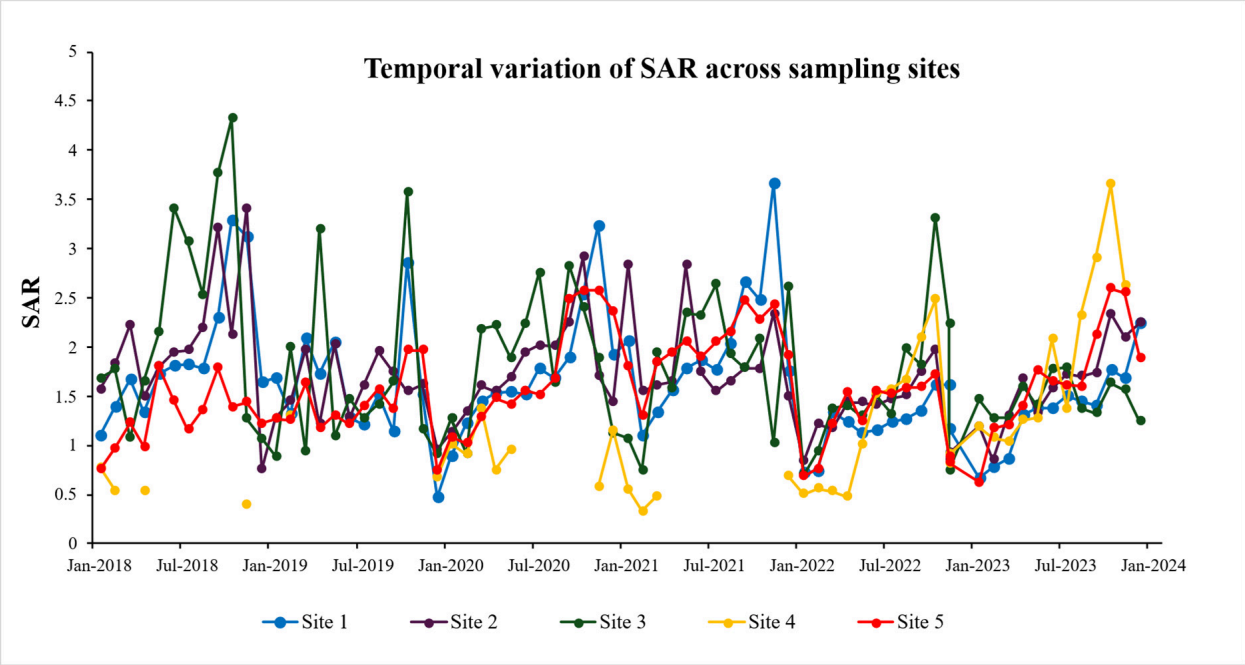
3.4. Spatial and Temporal Trends

Temporal trends analysis

Temporal trends for the WA-WQI, SAR, and Na% were analyzed across the five sampling sites to assess the changes over the monitoring period. The analysis allows for the identification of periods of deterioration or improvement in water quality, highlighting both episodic events and sustained trends influenced by anthropogenic and natural factors. The temporal trend results are presented in Figure 7.

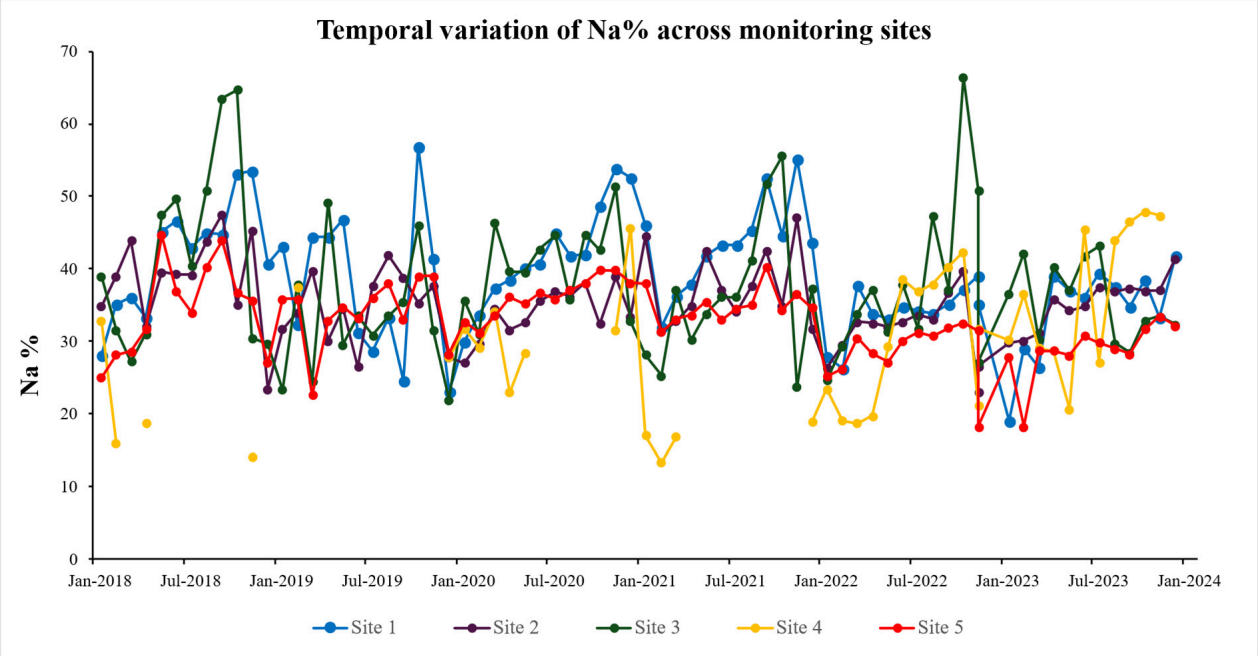


(**a**)



(**b**)

Figure 7. *Cont.*



(**c**)

Figure 7. Temporal variations in (**a**) WA-WQI, (**b**) SAR, and (**c**) Na% across sampling sites from 2018 to 2023.

The temporal trends for the WA-WQI across the sites are indicated in Figure 7a. The WA-WQI time series shows that deterioration peaked during 2019–2022, with frequent and extreme episodic spikes across Sites 3, 4, and 5. Although Sites 1 and 2 generally recorded lower WQI values, both experienced occasional contamination events. Conditions appeared to stabilize in 2023; however, the recurrence of extreme events underscores the catchment's continued susceptibility to anthropogenic pressures.

Figure 7b presents the SAR temporal trends across all sites. The SAR values for most sites were stable; however, a gradual increase has been evident at several sites after 2020, suggesting cumulative effects of land use and coal mining activities. The SAR patterns indicate that the natural buffering processes within the catchment currently mitigate Na-related impacts. However, localized anthropogenic activities appear to drive variability across the sites. Although present values remain within safe irrigation limits, episodic peaks highlight the potential for future sodicity risks should Na enrichment become more frequent or sustained.

The temporal trend analysis for Na% across all the sampling sites are presented in Figure 7c. Site 1 fluctuated widely with repeated short-term increases followed by decreases, indicating strong temporal variability. Episodic peaks above 50% occurred intermittently, suggesting periods of elevated sodicity influence. Site 2 was mostly stable across the monitoring period; however, peaks occurred during 2018–2019 and 2021–2022. Site 3 exhibited the highest temporal variability, characterized by sharp increases such as in September 2018 and October 2022, reflecting sporadic Na enrichment likely associated with upstream activities. At Site 4, Na% values remained relatively low and stable over time, although a slight increase was observed during 2022–2023, indicating seasonal or short-term influences. Temporal fluctuations at Site 5 were moderate, with occasional fluctuations.

Gibbs diagrams

The Gibbs diagrams were used to evaluate the dominant processes controlling the water chemistry at each monitoring point and to distinguish between the natural geochem-

ical processes and potential anthropogenic influences. The Gibbs diagrams for the five sampling sites are presented in Figure 8.

Site 1 (upstream) is characterized predominantly by rock–water interactions, suggesting that carbonate and silicate mineral weathering and the local geological setting are the primary controls on water chemistry. Although elevated concentrations of some parameters were observed at this site, the geochemical signature indicates that natural geological processes have a greater influence on the quality of water than potential anthropogenic inputs. The clustering of samples within the rock dominance and freshening zones further suggests that dilution from precipitation and surface water recharge plays a significant role in moderating salinity levels.

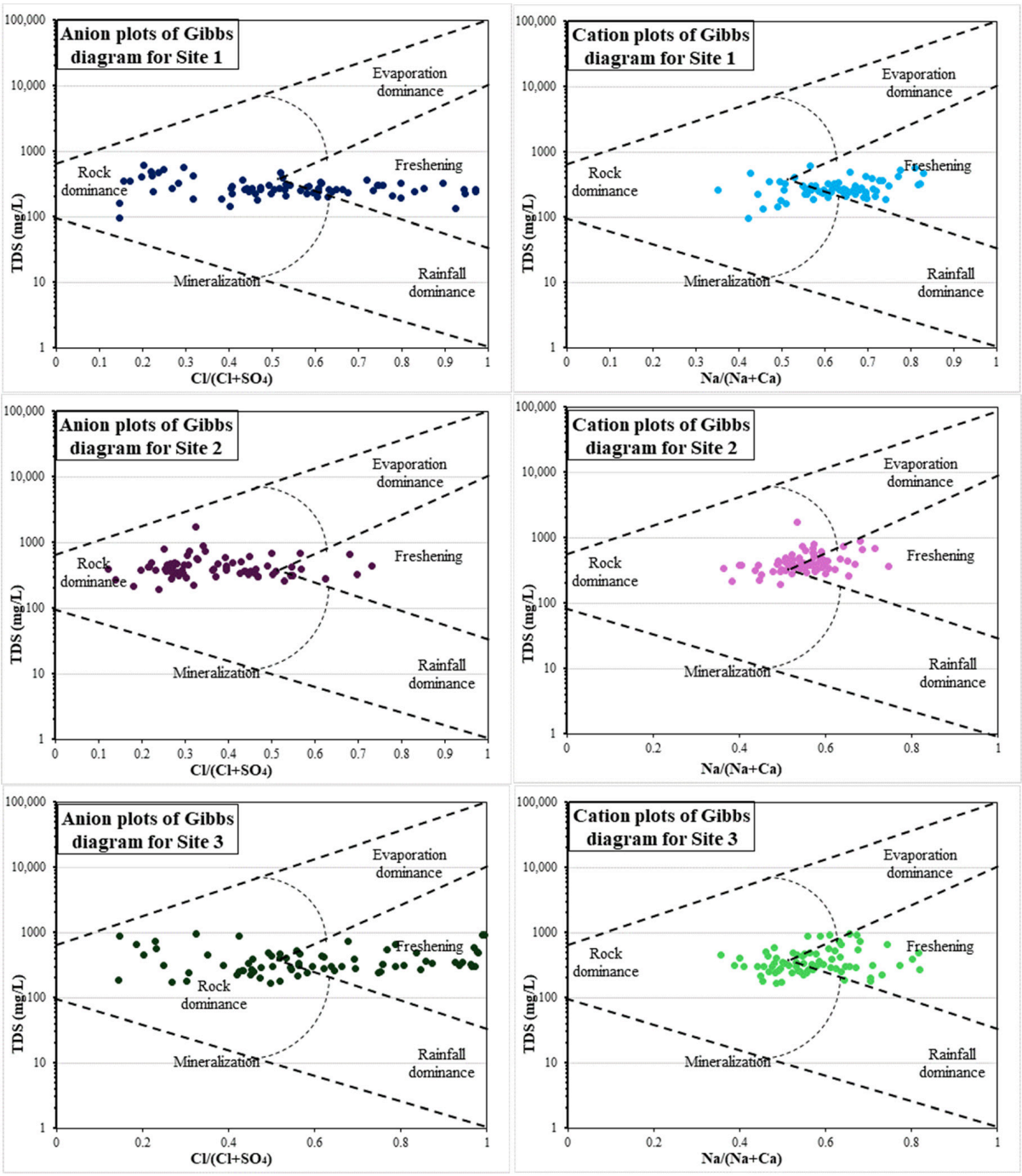


Figure 8. *Cont.*

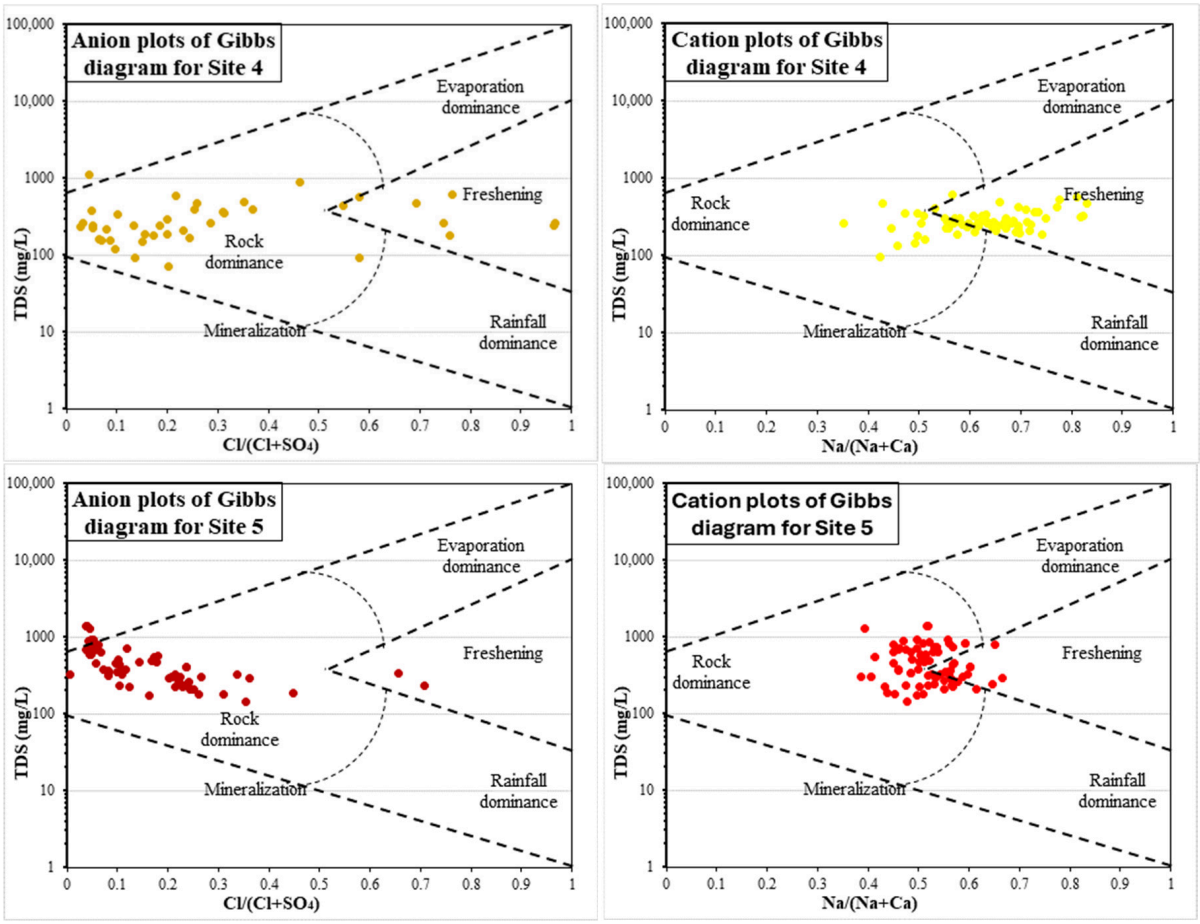


Figure 8. Gibbs Diagrams for monitoring Sites 1–5 showing anion and cation hydrochemical characteristics. Different colors distinguish the cation and anion datasets at each monitoring site.

Site 2 is characterized by elevated TDS and high Na and Cl ratios, indicating evaporative concentration processes and possible saline inputs. The shift of samples towards the evaporation–crystallization dominance zone suggests increasing salinity and progressive deterioration in water quality.

Site 3 exhibits a greater tendency towards the evaporation–crystallization dominance zone, particularly in the anion plot, where several samples display elevated Cl ratios indicative of evaporative enrichment. These hydrochemical characteristics are consistent with increased salinity and may reflect the combined influence of catchment activities, including mining and agriculture.

Site 4 indicates that water chemistry is influenced by a combination of rock-weathering and evaporation–crystallization processes. While most samples fall within the rock dominance field in the anion plot, several shift towards the freshening and evaporation zones, suggesting moderate salinity build-up that may be associated with anthropogenic influences. This indicates that Site 4 represents a transitional zone where natural geogenic processes and human activities collectively influence the water quality.

Site 5 is characterized by elevated salinity and greater influence of evaporation processes, as reflected by higher TDS and increased Na and Cl ratios. Given its downstream position, the site likely integrates cumulative inputs from upstream activities and natural geochemical processes.

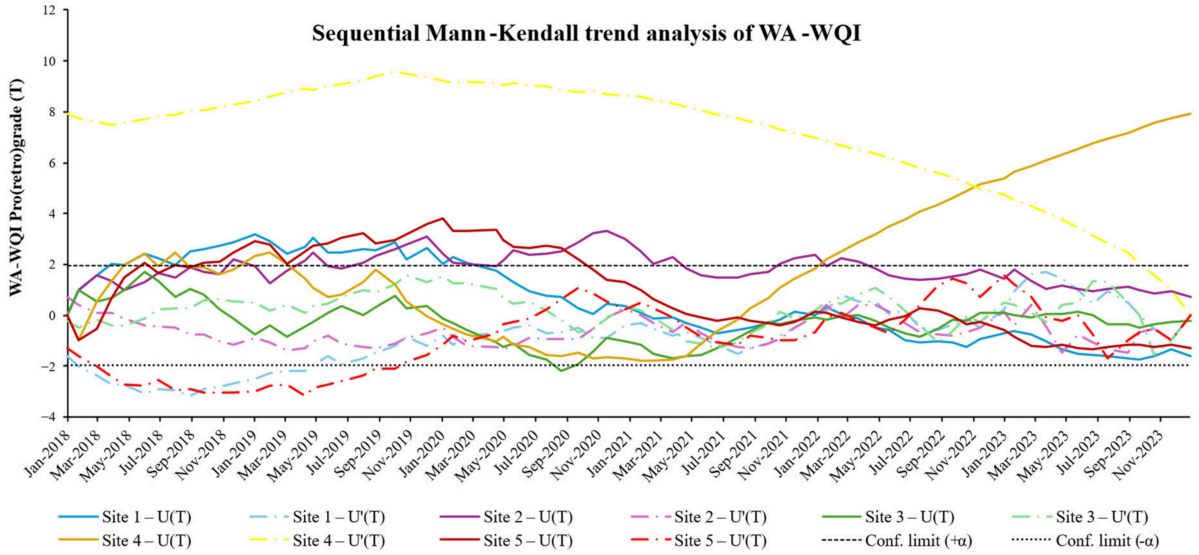
Overall, the Gibbs diagrams indicate that rock weathering and evaporation–crystallization processes are the principal mechanisms controlling the hydrochemistry of the Leeuwfonteinspruit. The progressive shift towards evaporation dominance at the downstream

sites coincides with areas influenced by mining and other land-use activities, suggesting that these factors may contribute to the observed salinity enrichment.

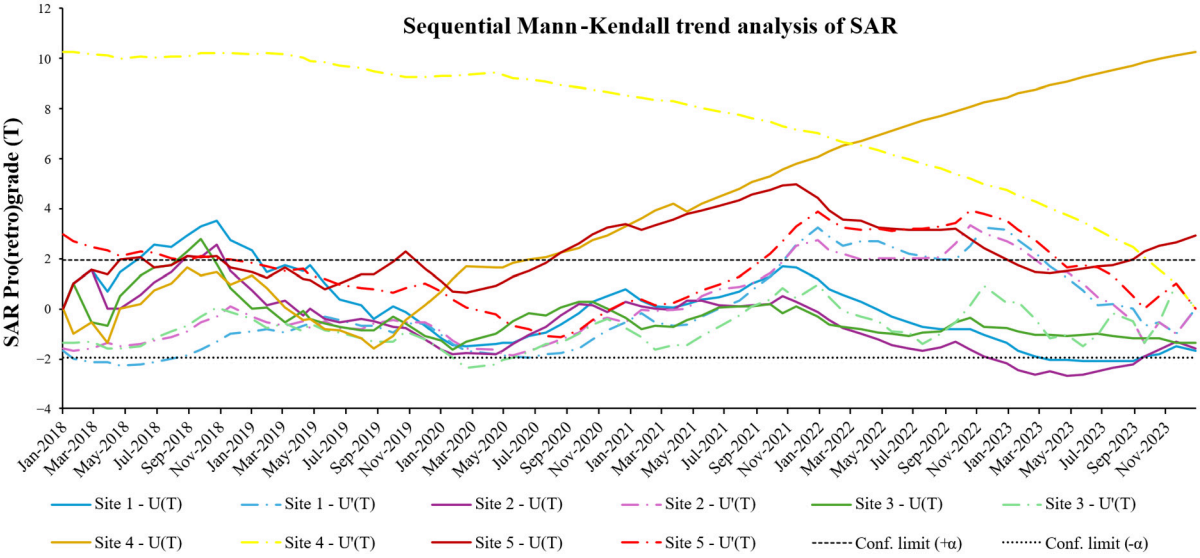
Sequential Mann–Kendall (SMK)

The SMK test was applied to evaluate temporal trends in WQI, SAR, and Na% across five sampling sites. The confidence limits were set at ±1.96, with values above +1.96 indicating a statistically significant increasing trend and values below −1.96 indicating a significant decreasing trend. The SMK results are presented in Figure 9.

For WQI (Figure 9a), site 1 indicated a temporary increase from 2018 to early 2019, followed by stabilization and fluctuations around the baseline, indicating no significant monotonic trend. Site 2 exceeded the confidence limit between 2019 and mid-2021, before stabilizing between 2022 and 2023. Site 3 fluctuated throughout the monitoring period without a clear monotonic trend. Site 4 displayed a pronounced and persistent increasing trend from May 2021, indicating progressive water quality deterioration. Site 5 exhibited an increasing trend from 2019 to 2020 before stabilizing around the baseline after 2021.

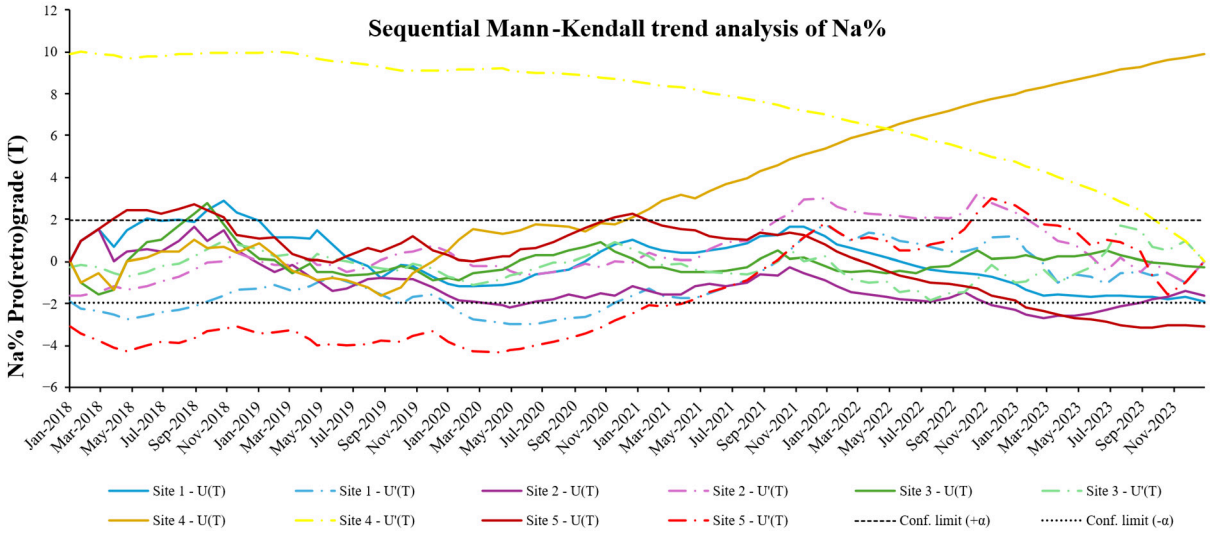


(**a**)



(**b**)

Figure 9. *Cont.*



(**c**)

Figure 9. Sequential Mann–Kendall trends of (**a**) WA-WQI, (**b**) SAR and (**c**) Na% across sampling sites from 2018 to 2023.

For SAR (Figure 9b), the upstream Sites (1–3) largely remained within the confidence limits. These sites exhibited early increases during 2018, followed by declines until March 2020. Site 1 subsequently fluctuated without a significant monotonic trend, while Site 2 indicated temporary variability during 2021–2022 followed by a decreasing trend from 2022 to December 2023, suggesting reduced sodicity risks, possibly due to dilution or reduced saline inflows. Site 3 followed a similar pattern and remained relatively stable. In contrast, Site 4 indicated a statistically significant increasing trend beginning in 2020 and continuing steeply until December 2023, representing the strongest SAR increase across all sites. Site 5 was initially stable from 2018 to 2019, but from 2020 onwards showed a sustained increasing trend, exceeding the confidence limit in September 2020 and remaining elevated until December 2022. Despite temporary stabilization in early 2023, SAR levels resumed an upward trend towards the end of the monitoring period.

For Na% (Figure 9c), Sites 1 and 3 exhibited short-term variability, characterized by temporary increases in 2018 followed by decreases in 2019 and 2020, and subsequent oscillations around the baseline, indicating no significant monotonic trend. Site 2 displayed a gradual decreasing trend during the latter part of the monitoring period, with values approaching or exceeding the lower confidence limit by 2023. In contrast, Site 4 exhibited a strong and sustained positive trend, with marked intensification after 2020, indicating progressive Na enrichment. Site 5 indicated increasing tendencies during the early monitoring period (2018–2020) but shifted into a decreasing trend from 2021 onwards, suggesting temporal changes in Na dynamics at this site.

Overall, the SMK analysis indicates that water quality trends in the Leeuwfonteinspruit are characterized by relatively stable conditions at Sites 1–3, where short-term fluctuations occurred without persistent monotonic trends. In contrast, Site 4 consistently displayed the strongest and most consistent increasing trends across WQI, SAR, and Na% after 2020, indicating progressive deterioration in water quality and irrigation suitability. Site 5 showed evidence of temporal variability, with initial deterioration followed by partial stabilization and subsequent fluctuations. Collectively, these findings demonstrate that while the upper reaches of the catchment exhibit a degree of resilience, certain locations, particularly Site 4 and Site 5, are more susceptible to long-term degradation.

3.5. Principal Component Analysis

The PCA results reveal the strong data suitability for dimensionality reduction across all sites, as indicated by Kaiser–Meyer–Olkin values with a score of 0.69 at Site 1, 0.83 at Site 2, 0.77 at Site 3, 0.70 at Site 4, and 0.77 at Site 5. These values suggest that the correlation patterns among water quality variables were sufficient to extract the meaningful principal components. The rotated component matrix further demonstrates that certain parameters group together strongly at each sampling site, indicating similar hydrochemical behavior and potentially common controlling processes.

Across the five monitoring sites, the PCA revealed that the majority of water quality variability is explained by a limited number of components with eigenvalues greater than 1 (Table 6). Site 1 extracted six components accounting for 81.2% of variance, Site 2 extracted four components explaining 80.8%, Site 3 extracted six components explaining 82.3%, Site 4 extracted six components explaining 83.8%, and Site 5 extracted five components explaining 83.2%. Table 7 presents the rotated component matrix of squared variable loadings for all the sampling sites, rotated with Varimax and Kaiser Normalization.

Table 6. Summary of the principal axis factoring for Sites 1–5 (components with eigenvalues > 1).

Sampling Sites	Component	Initial Eigenvalues			Rotation Sums of Squared Loadings		
		Total	% of Variance	Cumulative %	Total	% of Variance	Cumulative %
Site 1	1	6.77	35.64	35.64	5.83	30.68	30.68
	2	2.53	13.32	48.95	2.32	12.23	42.91
	3	2.14	11.25	60.85	2.18	11.47	54.38
	4	1.83	9.65	69.85	2.13	11.21	65.59
	5	1.15	6.05	75.90	1.94	10.19	75.78
	6	1.00	5.28	81.18	1.03	5.40	81.18
Site 2	1	9.27	48.81	48.81	8.77	46.16	46.16
	2	3.10	16.29	65.10	3.06	16.09	62.24
	3	1.85	9.73	74.83	2.38	12.55	74.79
	4	1.13	5.96	80.79	1.14	6.00	80.79
Site 3	1	8.07	42.46	42.46	7.30	38.41	38.41
	2	2.35	12.37	54.83	2.36	12.39	50.80
	3	1.77	9.33	64.17	2.09	10.98	61.78
	4	1.20	6.31	70.48	1.44	7.60	69.37
	5	1.14	6.00	76.47	1.27	6.69	76.06
	6	1.10	5.79	82.26	1.18	6.20	82.26
Site 4	1	7.63	40.16	40.16	5.89	30.99	30.99
	2	3.10	16.29	56.45	3.97	20.89	51.87
	3	1.78	9.35	65.80	2.51	13.23	65.10
	4	1.39	7.33	73.12	1.43	7.51	72.61
	5	1.03	5.40	78.52	1.10	5.77	78.38
	6	1.01	5.29	83.81	1.03	5.43	83.81
Site 5	1	7.44	39.18	39.18	7.15	37.65	37.65
	2	3.53	18.59	57.76	3.13	16.45	54.10
	3	1.93	10.16	67.92	2.16	11.39	65.49
	4	1.85	9.73	77.65	2.05	10.78	76.27
	5	1.06	5.57	83.22	1.32	6.95	83.22

Table 7. Rotated component matrix of squared variable loadings for Site 1–5.

Sites	Component	Variables																	
		Turbidity	Na	EC	TDS	K	SO_4	Mg	pH	N	Ca	SS	Al	Fe	Cl	F	Alk	Mn	PO_4	Hardness
Site 1	1		0.94	0.89	0.88	0.79	0.69	0.67	0.61						0.95					0.52
	2						0.44			0.73	0.65	0.61								0.53
	3	0.66											0.87	0.76						
	4											0.42				0.87	0.82			
	5							0.47			0.57							0.78		0.57
	6																		0.96	
Site 2	1		0.86	0.94	0.97	0.60	0.85	0.97			0.92			0.64	0.92		0.60	0.84		0.98
	2	0.94				0.51						0.90	0.74	0.49		0.41				
	3								0.72							0.74	0.60			
	4																		0.96	
Site 3	1		0.87	0.96	0.96	0.80	0.55	0.92			0.77				0.87		0.62	0.26		0.89
	2													0.54		0.54	0.64	0.83		
	3	0.78								0.46			0.74	0.58						
	4											0.87				0.48				
	5								0.74	0.59										
	6																		0.90	
Site 4	1		0.48	0.75	0.88		0.94	0.82			0.93							0.81		0.91
	2		0.83	0.63					0.63						0.88		0.86			
	3	0.76								0.84			0.55						0.83	
	4					0.69								0.91						
	5											0.97								
	6															0.98				
Site 5	1		0.93	0.98	0.98		0.97	0.96	0.53		0.97									0.98
	2											0.52					0.93	0.93	0.90	
	3					0.85									0.56	0.88				
	4												0.96	0.92						
	5	0.62									0.77	0.49								

The PCA results across the five sampling sites reveal patterns indicating that salinity and mineralization processes are among the dominant factors influencing water quality within the Leeuwfonteinspruit. Parameters such as TDS, EC, SO_4, Na, Mg, Ca, and hardness were persistently associated with the first principal component at all sites, suggesting a common geochemical behavior associated with ionic enrichment and dissolved solids. These associations may reflect a combination of natural weathering processes and anthropogenic influences within the catchment, including mining activities.

Upstream sites (Sites 1 and 2) reflected relatively stronger natural geochemical signatures, with secondary contributions associated with nutrients and suspended solids, which may indicate diffuse inputs from agricultural activities, soil erosion, and other land use activities. In contrast, Sites 3–5 exhibited stronger associations between salinity-related parameters and heavy metals such as Mn, Fe and Al, patterns that are consistent with potential mining influences and cumulative upstream inputs.

The occurrence of nutrient-related parameters (N and PO_4) and SS in higher-order components across multiple sites further suggests episodic agricultural runoff, domestic effluent discharge, and sediment mobilization. Overall, the PCA results demonstrate a progressive downstream intensification of anthropogenic influences, where mining, agriculture, and natural processes interact synergistically to shape the spatial variation in surface water quality within Leeuwfonteinspruit.

3.6. Correlation Analysis

The correlation analysis for the selected physicochemical parameters was conducted to determine the relationships and differences between the parameters (Figure 10). The results indicate a strong positive relationship ($r > 0.9$) among several key physicochemical parameters. The strongest correlation was observed between TDS and EC ($r = 0.98$), which was expected as TDS directly influences the EC by increasing the concentration of ions in solution [28]. Similarly, TDS exhibited strong positive correlations with Mg ($r = 0.96$) and Ca ($r = 0.96$), indicating that these divalent cations are major contributors to the dissolved solids in the system. Both Mg and Ca also correlated strongly with EC ($r = 0.97$ and $r = 0.93$, respectively), further confirming their influence on water conductivity. Na

followed the same pattern, with a high correlation with EC (r = 0.95). The strong association between Mg and Ca (r = 0.92) suggests a shared source, likely linked to carbonate and silicate weathering.

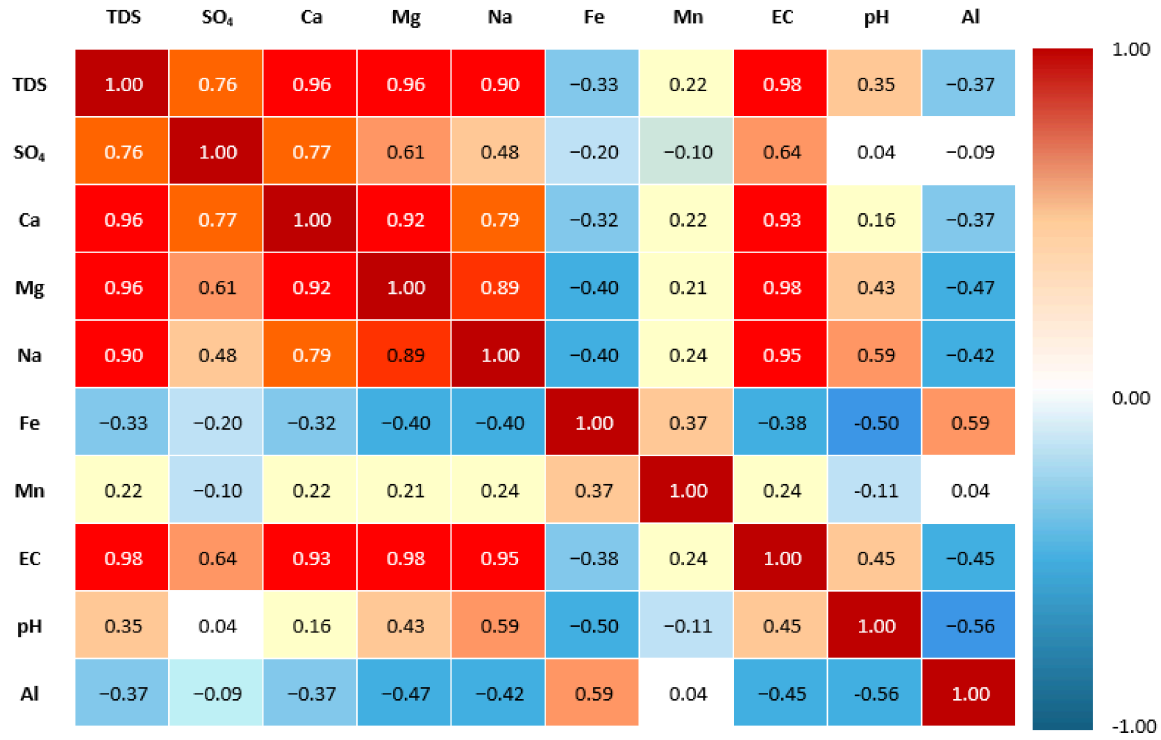


Figure 10. Correlation heat map for the selected water quality variables (key indicators of coal mining impacts).

In contrast, notable negative correlations (r < −0.4) were observed between pH and certain metals, particularly Fe and Al. The inverse relationship between Fe and pH (r = −0.50) suggests that Fe concentrations tend to be higher in more acidic conditions, due to increased solubility [58]. A similar pattern was evident for Al, which also indicated a strong negative correlation with pH (r = −0.56). These relationships are consistent with known geochemical behavior of these metals under low pH conditions, such as those found in mine-influenced drainage areas. Additionally, weaker negative correlations were observed between TDS and Al (r = −0.37) and between Mg and Al (r = −0.47), implying that Al may originate from different geochemical processes than those contributing to general salinity and water hardness.

Iron (Fe) exhibited weak or negative correlations with most parameters, indicating that its mobility is primarily controlled by pH and redox conditions rather than ionic load. Additionally, Mn showed weak to moderate positive correlations with TDS and EC, although its behavior was less consistent, suggesting localized redox variability. SO_4 exhibited a moderate correlation with TDS (r = 0.76) and weaker correlations with Ca and Mg, indicating that while it contributes to the dissolved solids, its role is secondary compared with the dominant influence of major cations.

4. Conclusions and Recommendations

This study provided a comprehensive assessment of surface water quality in the Leeuwfonteinspruit, a tributary of the Olifants River, over the period 2018–2023. Through the integration of guideline-based assessments, water quality indices, hydrochemical tools, and multivariate statistical analyses, the study evaluated the current water quality status,

identified spatial and temporal trends, and investigated potential sources and pathways of contamination.

The results indicate a progressive deterioration in water quality from upstream to downstream sites, with most pronounced deterioration observed at Site 5. Elevated TDS, EC, SO_4, Ca, Mg, Mn, Fe, and Al, together with poor to marginal WQI classifications, suggest substantial anthropogenic influence and potential contributions from mining-influenced drainage, despite generally neutral pH conditions. While most parameters remained within livestock water quality guidelines, frequent exceedances of domestic, aquatic ecosystem, and irrigation guidelines indicate potential risks to downstream water users and ecosystem health. Irrigation assessments based on SAR, Na%, and the USSL diagram indicated that the surface water generally poses a low sodicity hazard, with all samples classified within the S1 category. However, the predominance of the C2–S1 and C3–S1 classes indicates that irrigation suitability is primarily constrained by salinity rather than sodium accumulation, suggesting that appropriate salinity management practices may be required where elevated salinity conditions occur.

Spatial analyses demonstrated a transition from predominantly geogenic controls at upstream sites to increasing anthropogenic influence downstream. The occurrence of water quality degradation at Sites 3 and 4, which are situated upstream of the immediate study area, further suggests that additional pressures, including agriculture, other mining activities, and natural geochemical processes, may also contribute to the observed water quality patterns. Similarly, temporal analyses indicated periods of pronounced deterioration between 2019 and 2022, coinciding with intensified mining activities and hydrological variability, followed by partial but unstable recovery during 2022–2023.

Hydrochemical and multivariate statistical analyses suggested that water quality variability is largely associated with salinity and mineralization processes that may be influenced by mining activities, with secondary contributions from agricultural and other catchment sources. The findings therefore indicate that opencast coal mining is likely an important contributor to surface water quality deterioration in the Leeuwfonteinspruit, although the observed patterns reflect the combined influence of multiple anthropogenic and natural drivers. Overall, the study highlights the importance of integrated monitoring and adaptive management strategies to protect water resources within heavily mined catchments.

Recommendations and mitigation strategies

The following recommendations are proposed to mitigate the impacts of coal mining on the Leeuwfonteinspruit and protect downstream water users:

- Targeted management of key contaminants: Priority intervention should focus on the dominant contaminants identified in the study, including salinity-related parameters (TDS, EC, SO4, Ca and Mg) and trace metals (Fe, Mn, and Al). Appropriate treatment and mitigation measures should aim to limit metal mobilization and reduce salinity enrichment in the Leeuwfonteinspruit.
- Control of sources and pathways of contamination: Pollution prevention measures should address potential contamination pathways, including mine water discharges, seepage from pollution control facilities and discard dumps, and runoff from disturbed mining areas. Measures such as improved lining of pollution control dams, seepage interception systems, and rehabilitation of contaminated drainage pathways should be prioritized.
- Stormwater and mine water management: Clean and dirty water systems must be strictly separated. Clean stormwater should be diverted away from disturbed areas (such as active mining zones, coal stockpiles, carbonaceous material storage areas, discard dumps, haul roads, wash bays, workshops, and loading/offloading zones),

while contaminated water should be contained in lined pollution control dams for treatment, reuse, or compliant discharges. This is critical during high-risk temporal periods, particularly wet seasons and high-runoff events.

- Temporal risk management and adaptive monitoring: Monitoring and management strategies should explicitly account for periods of elevated risk, particularly during intensified mining phases and hydrologically sensitive periods. Adaptive monitoring programs should be implemented to increase sampling frequency during high-risk periods to allow early detection and rapid management response to episodic contamination events.
- Protection of vulnerable downstream users: Management interventions must prioritize downstream user vulnerabilities, including domestic water users, agricultural users (irrigation and livestock), and aquatic ecosystems. This includes improving water treatment for community use and ensuring ecological flow and quality requirements are maintained to protect aquatic biodiversity.
- Regulatory enforcement: Relevant authorities (DWS) should strengthen regulatory enforcement measures to ensure that the coal mining operations are held accountable for the degradation of water resources. This includes conducting regular inspections, ensuring compliance with water use licenses and environmental management plans, and imposing penalties or remediation requirements on mines found to be contributing to water pollution.
- Progressive rehabilitation: Active and disturbed mining areas should undergo concurrent rehabilitation to restore ecosystem functions, reduce long-term pollution risks, limit contaminant mobilization, and ensure post-mining land use sustainability.
- Integrated catchment management: An integrated catchment management approach should be implemented to effectively address cumulative impacts from mining, agriculture, domestic activities, and other land uses.

Author Contributions: Conceptualization, C.M.M.; methodology, C.M.M.; software, C.M.M.; validation, C.M.M., G.B. and P.O.; formal analysis, C.M.M.; investigation, C.M.M.; data curation, C.M.M.; writing—original draft preparation, C.M.M.; writing—review and editing, C.M.M., G.B. and P.O.; supervision, G.B. and P.O.; project administration, C.M.M., G.B. and P.O.; funding acquisition, C.M.M. All authors have read and agreed to the published version of the manuscript.

Funding: This research received funding from Centre for Graduate Support, University of the Free State (no specific grant number available) and Geovicon Environmental (Pty) Limited.

Data Availability Statement: The data presented in this study are available on request from the corresponding author, subject to reasonable request and applicable confidentiality restrictions.

Acknowledgments: The authors acknowledge the University of the Free State, particularly the Centre for Environmental Management, for providing the academic platform and resources supporting this study, as well as the Centre for Graduate Support for financial assistance. Appreciation is extended to Geovicon Environmental (Pty) Ltd. and its management for providing access to data and for their technical and financial support. The authors also thank colleagues, friends, and family for their encouragement and assistance throughout the study.

Conflicts of Interest: The authors declare that this study received funding from Geovicon Environmental (Pty) Limited. The funders had no role in the design of the study; in the collection, analyses, or interpretation of data; in the writing of the manuscript; or in the decision to publish the results.

Abbreviations

The following abbreviations are used in this manuscript:

Al	Aluminum
Ca	Calcium
CCME-WQI	Canadian Council of Ministers of the Environment Water Quality Index
Cl	Chloride
DWAF	Department of Water Affairs and Forestry
DWS	Department of Water and Sanitation
EC	Electrical Conductivity
F	Fluoride
Fe	Iron
ICP-MS	Inductively Coupled Plasma–Mass Spectrometry
ICP-OES	Inductively Coupled Plasma–Optical Emission Spectrometry
K	Potassium
meq/L	Milliequivalents per liter
Mg	Magnesium
mg/L	Milligrams per liter
Mn	Manganese
N	Nitrate and nitrite
Na	Sodium
Na%	Sodium percentage
PCA	Principal Component Analysis
PO_4	Phosphate
SAR	Sodium Adsorption Ratio
SAWQG	South African Water Quality Guidelines
SMK	Sequential Mann–Kendall
SO_4	Sulphate
SS	Suspended Solids
TDS	Total Dissolved Solids
TWQR	Target Water Quality Range
USSL	United States Salinity Laboratory
WA-WQI	Weighted Arithmetic Water Quality Index
WQI	Water Quality Index

References

1. International Energy Agency (IEA). World Energy Outlook 2024. 2024. Available online: https://www.iea.org/reports/world-energy-outlook-2024 (accessed on 9 January 2025).
2. Bulmer, E.; Pela, K.; Eberhard-Ruiz, A.; Montoya, J. *Global Perspective on Coal Jobs and Managing Labor Transition out of Coal*; World Bank: Washington, DC, USA, 2021; Volume 3, p. 21. Available online: https://documents1.worldbank.org/curated/en/099415103242235561/pdf/P1711940ae202d0cc09c1301e5b09e6e876.pdf (accessed on 20 May 2024).
3. Acharya, B.S.; Kharel, G. Acid mine drainage from coal mining in the United States–An overview. *J. Hydrol.* **2020**, *588*, 125061. [CrossRef]
4. Dontala, S.P.; Reddy, T.B.; Vadde, R. Environmental aspects and impacts its mitigation measures of corporate coal mining. *Procedia Earth Planet. Sci.* **2015**, *11*, 2–7. [CrossRef]
5. Mbedzi, M.D.; van der Poll, H.M.; van der Poll, J.A. Enhancing a decision-making framework to address environmental impacts of the South African coalmining industry. *Energies* **2020**, *13*, 4897. [CrossRef]
6. Kamble, P.H.; Kumbhar, J.S. An overview of impact of coal mining on water resources. *Int. J. Sci. Res. Multidiscip. Stud.* **2019**, *5*, 115–121. Available online: https://www.researchgate.net/publication/338570899 (accessed on 20 February 2024).
7. Kumar, M.; Srivastava, M.K.; Kishor, K.; Singh, A.K. An Assessment of the Environmental Impact of Coal Mining through Acid Mine Drainage and Soil Degradation from Makum Coalfields, Upper Assam, India: A Case Study. *J. Geol. Soc. India* **2023**, *99*, 1113–1120. [CrossRef]

8. Finkelman, R.B.; Wolfe, A.; Hendryx, M.S. The future environmental and health impacts of coal. *Energy Geosci.* **2021**, *2*, 99–112. [CrossRef]
9. Nunes, L.J. The rising threat of atmospheric CO_2: A review on the causes, impacts, and mitigation strategies. *Environments* **2023**, *10*, 66. [CrossRef]
10. Masood, N.; Hudson-Edwards, K.; Farooqi, A. True cost of coal: Coal mining industry and its associated environmental impacts on water resource development. *J. Sustain. Min.* **2020**, *19*, 135–149. [CrossRef]
11. Munawer, M.E. Human health and environmental impacts of coal combustion and post-combustion wastes. *J. Sustain. Min.* **2018**, *17*, 87–96. [CrossRef]
12. Zhou, M.; Li, X.; Zhang, M.; Liu, B.; Zhang, Y.; Gao, Y.; Ullah, H.; Peng, L.; He, A.; Yu, H. Water quality in a worldwide coal mining city: A scenario in water chemistry and health risks exploration. *J. Geochem. Explor.* **2020**, *213*, 106513. [CrossRef]
13. Ekwule, O.R.; Akpen, G.D.; Ugbede, G.M. The effect of coal mining on the water quality of water sources in Nigeria. *Bartın Univ. Int. J. Nat. Appl. Sci.* **2019**, *2*, 251–260. Available online: https://www.researchgate.net/publication/344391020 (accessed on 13 April 2024).
14. Wright, I.A.; Belmer, N.; Davies, P.J. Coal mine water pollution and ecological impairment of one of Australia's most 'protected' high conservation-value rivers. *Water Air Soil Pollut.* **2017**, *228*, 90. [CrossRef]
15. Moyo, A.; Do Amaral Filho, J.R.; Harrison, S.T.; Broadhurst, J.L. Acid mine drainage and metal (loid) risk potential of South African coal processing wastes. *Miner. Eng.* **2024**, *215*, 108825. [CrossRef]
16. Esterhuyse, S.; Buschke, F. Coal and Water: Exploiting One Precious Natural Resource at the Expense of Another? In *Coal and Energy in South Africa*; Edinburgh University Press: Edinburgh, UK, 2022; pp. 88–90. Available online: https://www.jstor.org/stable/10.3366/jj.7358700.15 (accessed on 22 August 2025).
17. Ray, S.; Dey, K. Coal mine water drainage: The current status and challenges. *J. Inst. Eng. Ser. D* **2020**, *101*, 165–172. [CrossRef]
18. Mnyango, S.S.; Thwala, M.; Oberholster, P.J.; Truter, C.J. Using multiple indices for the water resource management of a monomictic man-made dam in Southern Africa. *Water* **2022**, *14*, 3366. [CrossRef]
19. Hanto, J.; Schroth, A.; Krawielicki, L.; Oei, P.Y.; Burton, J. South Africa's energy transition–unraveling its political economy. *Energy Sustain. Dev.* **2022**, *69*, 164–178. [CrossRef]
20. Hassan, A.S. Coal mining and environmental sustainability in South Africa: Do institutions matter? *Environ. Sci. Pollut. Res.* **2022**, *30*, 20431–20449. [CrossRef] [PubMed]
21. Simpson, G.B.; Badenhorst, J.; Jewitt, G.P.; Berchner, M.; Davies, E. Competition for land: The water-energy-food nexus and coal mining in Mpumalanga Province, South Africa. *Front. Environ. Sci.* **2019**, *7*, 86. [CrossRef]
22. Oberholster, P.F.; Goldin, J.; Xu, Y.; Kanyerere, T.; Oberholster, P.J.; Botha, A.M. Assessing the adverse effects of a mixture of AMD and sewage effluent on a sub-tropical dam situated in a nature conservation area using a modified pollution index. *Int. J. Environ. Res.* **2021**, *15*, 321–333. [CrossRef]
23. Association for Water and Rural Development (AWARD). The role of the Wilge River in maintaining ecosystem integrity and associated benefits in the upper Olifants Catchment. In *Association for Water and Rural Development*; The Association for Water and Rural Development Location: Hoedspruit, South Africa, 2017; pp. 1–39. Available online: https://cer.org.za/wp-content/uploads/2017/09/Annexure-G-Role-of-the-Wilge-AWARD-Sep-2017.pdf (accessed on 11 April 2024).
24. Ngwenyama, P.L.; de Graaf, W.W. Risks and challenges affecting opencast pillar mining in previously mined underground bord and pillar workings. *J. South. Afr. Inst. Min. Metall.* **2021**, *121*, 623–631. [CrossRef]
25. Ratshomo, K.; Nembahe, R. *South African Energy Sector Report*; Department of Energy South Africa: Pretoria, South Africa, 2018; pp. 1–25.
26. Laisani, J.; Jegede, A.O. Impacts of coal mining in Witbank, Mpumalanga province of South Africa: An eco-legal perspective. *J. Rev. Glob. Econ.* **2019**, *8*, 1586–1597. [CrossRef]
27. Singh, G.; Pal, A.; Niranjan, R.K.; Kumar, M. Assessment of environmental impacts by mining activities: A case study from Jhansi open cast mining site-Uttar Pradesh, India. *J. Exp. Sci.* **2010**, *1*, 9–13.
28. Basharat, U.; Zhang, W.; Abbasi, A.; Mahroof, S.; Han, C.; Khan, S.H.; Li, S. Integrated assessment of groundwater hydrogeochemistry and quality using multivariate statistical analysis, self-organizing maps, and water quality indices in District Bagh, AJK, Pakistan. *Ecotoxicol. Environ. Saf.* **2025**, *301*, 118515. [CrossRef] [PubMed]
29. Iji, O.T.; Njoya, E.M.; Madikizela, B.; Myburgh, J.G.; McGaw, L.J. Evaluation of the genotoxic potential of water impacted by acid mine drainage from a coal mine in Mpumalanga, South Africa, using the Ames test and Comet assay. *Water SA* **2021**, *47*, 456–465. [CrossRef]
30. Monira, U.; Sattar, G.S.; Mostafa, M.G. Assessment of surface water quality using the Water Quality Index (WQI) and multivariate statistical analysis (MSA), around tannery industry effluent discharge areas. *H2Open J.* **2024**, *7*, 130–148. [CrossRef]
31. Owolabi, S.T.; Belle, J.A. Investigating extreme hydrological risk impact on water quality; evidence from Buffalo catchment headwater, Eastern Cape, South Africa. *Environ. Sci. Pollut. Res.* **2023**, *30*, 73425–73450. [CrossRef] [PubMed]

32. Rawat, K.S.; Singh, S.K.; Gautam, S.K. Assessment of groundwater quality for irrigation use: A peninsular case study. *Appl. Water Sci.* **2018**, *8*, 233. [CrossRef]
33. Akiner, M.E.; Chauhan, P.; Singh, S.K. Evaluation of Surface Water Quality in the Betwa River Basin through the Water Quality Index Model and Multivariate Statistical Techniques. *Environ. Sci. Pollut. Res.* **2024**, *31*, 18871–18886. [CrossRef] [PubMed]
34. Maremane, S.; Belle, G.; Oberholster, P. Assessment of effluent wastewater quality and the application of an integrated wastewater resource recovery model: The Burgersfort wastewater resource recovery case study. *Water* **2024**, *16*, 608. [CrossRef]
35. Dzhangi, T.R.; Atangana, E. Evaluation of the impact of coal mining on surface water in the Boesmanspruit, Mpumalanga, South Africa. *Environ. Earth Sci.* **2024**, *83*, 159. [CrossRef]
36. Han, X.; Tang, F.; Liu, A.L. Drinking water quality evaluation in supply systems in Wuhan, China: Application of entropy weight water quality index and multivariate statistical analysis. *Environ. Sci. Pollut. Res.* **2023**, *31*, 280–292. [CrossRef] [PubMed]
37. Piroozfar, P.; Alipour, S.; Modabberi, S.; Cohen, D. Using multivariate statistical analysis in assessment of surface water quality and identification of heavy metal pollution sources in Sarough watershed, NW of Iran. *Environ. Monit. Assess.* **2021**, *193*, 564. [CrossRef] [PubMed]
38. Atangana, E.; Oberholster, P.J. Using heavy metal pollution indices to assess water quality of surface and groundwater on catchment levels in South Africa. *J. Afr. Earth Sci.* **2021**, *182*, 104254. [CrossRef]
39. Lebepe, J.; Oberholster, P.J.; Ncube, I.; Smit, W.; Luus-Powell, W.J. Metal levels in two fish species from a waterbody impacted by metallurgic industries and acid mine drainage from coal mining in South Africa. *J. Environ. Sci. Health Part A* **2019**, *55*, 421–432. [CrossRef] [PubMed]
40. Oberholster, P.J.; Botha, A.M.; Hill, L.; Strydom, W.F. River catchment responses to anthropogenic acidification in relationship with sewage effluent: An ecotoxicology screening application. *Chemosphere* **2017**, *189*, 407–417. [CrossRef] [PubMed]
41. Dabrowski, J.M.; Dabrowski, J.; Hill, L.; Macmillan, P.; Oberholster, P.J. Fate, transport and effects of pollutants originating from acid mine drainage in the Olifants River, South Africa. *River Res. Appl.* **2014**, *31*, 1354–1364. [CrossRef]
42. da Silva Bonifácio, A.; de Lima Brum, R.; Tavella, R.A.; Ramires, P.F.; Lessa, I.M.; Dos Santos, M.; da Silva Júnior, F.M.R. Human health risk assessment of metals and anions in surface water from a mineral coal region in Brazil. *Environ. Monit. Assess.* **2021**, *193*, 567. [CrossRef] [PubMed]
43. Prathap, A.; Chakraborty, S. Assessment of surface water quality around opencast coal mines for sustainable utilization potentials: A case study in Jharkhand, India. *Environ. Dev. Sustain.* **2019**, *22*, 3179–3205. [CrossRef]
44. Department of Water Affairs and Forestry. *South African Water Quality Guidelines*, 2nd ed.; Volume 1: Domestic Use; Department of Water Affairs and Forestry: Pretoria, South Africa, 1996. Available online: https://www.dws.gov.za/iwqs/wq_guide/Pol_saWQguideFRESHDomesticusevol1.PDF (accessed on 22 August 2025).
45. Department of Water Affairs and Forestry. *South African Water Quality Guidelines*, 2nd ed.; Volume 4: Agricultural Use: Irrigation; Department of Water Affairs and Forestry: Pretoria, South Africa, 1996. Available online: https://www.dws.gov.za/iwqs/wq_guide/edited/Pol_saWQguideFRESHIrrigationvol4.pdf (accessed on 22 August 2025).
46. Department of Water Affairs and Forestry. *South African Water Quality Guidelines*, 2nd ed.; Volume 5: Agricultural Use: Livestock Watering; Department of Water Affairs and Forestry: Pretoria, South Africa, 1996. Available online: https://www.dws.gov.za/iwqs/wq_guide/edited/Pol_saWQguideFRESH_vol5_Livestockwatering.pdf (accessed on 22 August 2025).
47. Department of Water Affairs and Forestry. *South African Water Quality Guidelines*, 2nd ed.; Volume 7: Aquatic Ecosystems; Department of Water Affairs and Forestry: Pretoria, South Africa, 1996. Available online: https://www.dws.gov.za/iwqs/wq_guide/edited/Pol_saWQguideFRESH_vol7_Aquaticecosystems.pdf (accessed on 22 August 2025).
48. Atangana, E. An indices-based water quality model to evaluate surface water quality: A case study in Vaalwaterspruit, Mpumalanga, South Africa. *J. Afr. Earth Sci.* **2023**, *205*, 105001. [CrossRef]
49. El Bilali, A.; Taleb, A. Prediction of irrigation water quality parameters using machine learning models in a semi-arid environment. *J. Saudi Soc. Agric. Sci.* **2020**, *19*, 439–451. [CrossRef]
50. Richards, L.A. (Ed.) Diagnosis and Improvement of Saline and Alkali Soils. In *USDA Agriculture Handbook No. 60.*; United States Department of Agriculture: Washington, DC, USA, 1954.
51. Gibbs, R.J. Mechanisms controlling world water chemistry. *Science* **1970**, *170*, 1088–1090. [CrossRef] [PubMed]
52. Marandi, A.; Shand, P. Groundwater chemistry and the Gibbs Diagram. *Appl. Geochem.* **2018**, *97*, 209–212. [CrossRef]
53. Owolabi, S.T.; Belle, J.A.; Mazinyo, S. Quantifying intra-catchment streamflow processes and response to climate change within a climatic transitional zone: A case study of Buffalo catchment, Eastern Cape, South Africa. *Mathematics* **2022**, *10*, 3003. [CrossRef]
54. Sneyers, R. *On the Statistical Analysis of Series of Observations*; World Meteorological Organization: Geneva, Switzerland, 1990.
55. Bisai, D.; Chatterjee, S.; Khan, A.; Barman, N.K. Application of sequential Mann-Kendall test for detection of approximate significant change point in surface air temperature for Kolkata weather observatory, west Bengal, India. *Int. J. Curr. Res.* **2014**, *6*, 5319–5324. Available online: https://www.journalcra.com/sites/default/files/issue-pdf/4972.pdf (accessed on 26 June 2026).
56. Arkoç, O.; Ucar, S.; Ozcan, C. Assessment of impact of coal mining on ground and surface waters in Tozaklı coal field, Kırklareli, northeast of Thrace, Turkey. *Environ. Earth Sci.* **2016**, *75*, 514. [CrossRef]

57. Ayers, R.S.; Westcot, D.W. *Water Quality for Agriculture*; Food and Agriculture Organization of the United Nations: Rome, Italy, 1985; pp. 1–174.
58. Khomo, L.; Mosebi, S.; Ntushelo, K. Microbiological impacts of acid mine drainage on urban agriculture in Soweto, South Africa. *Sci. Afr.* **2023**, *23*, e02055. [CrossRef]

Disclaimer/Publisher's Note: The statements, opinions and data contained in all publications are solely those of the individual author(s) and contributor(s) and not of MDPI and/or the editor(s). MDPI and/or the editor(s) disclaim responsibility for any injury to people or property resulting from any ideas, methods, instructions or products referred to in the content.